

THE EFFECTS OF LONG-TERM SPINAL CORD INJURY ON THE URINARY BLADDER
WALL TISSUE MECHANICS

by

Kevin Khashayar Toosi

Doctor of Medicine, Mashad University of Medical Sciences, 1994

Bachelor of Science, University of Pittsburgh, 2003

Submitted to the Graduate Faculty of
The School of Engineering in partial fulfillment
of the requirements for the degree of
Master of Science

University of Pittsburgh

2006

UNIVERSITY OF PITTSBURGH

SCHOOL OF ENGINEERING

This thesis was presented

by

Kevin Khashayar Toosi

It was defended on

January 20, 2006

and approved by

Michael B. Chancellor, Professor and Surgeon, Department of Urology

Jiro Nagatomi, Assistant Professor, Department of Bioengineering, Clemson University

Thesis Advisor: Michael S. Sacks, Professor, Department of Bioengineering

THE EFFECTS OF LONG-TERM SPINAL CORD INJURY ON THE URINARY BLADDER WALL TISSUE MECHANICS

Kevin Khashayar Toosi, M.S.

University of Pittsburgh, 2006

Approximately 250,000 – 400,000 individuals in the United States have spinal cord injuries (SCI); urologic complications, including bladder dysfunction, are among the most common problems these patients encounter. Although extensive studies have been conducted on the effects of spinal cord injury on bladder function, the alterations in mechanical behavior and functional properties of the bladder wall tissue and the underlying mechanisms are not well understood. Using a rat model of SCI, it has been previously demonstrated that the bladder wall significantly remodeled in early stages after injury. The remodeling process included changes in mechanical properties, composition and structure of the bladder wall, and occurred as early as 10 days post-injury.

Based on the previous findings, it was hypothesized that the altered mechanical environment of the urinary bladder following spinal cord injury was the key signal for the changes in the tissue functional properties. In order to test this hypothesis and gain a better understanding of relationship between function and structure of bladder wall following SCI, the present study combined different experimental methods (including mechanical testing, biochemical assays and histomorphometry) to investigate changes in mechanical properties, as

well as alterations in composition and morphology of the bladder wall tissue at various time points up to 10 weeks after injury.

Changes in mechanical compliance and material class found during the biomechanical analyses clearly indicated that the bladder wall continuously remodels after spinal cord injury beyond the time point previously tested. The results of histomorphometric study corroborated the mechanical data and provided first evidence that directional bladder smooth muscle cell hypertrophy was probably a major factor in determining changes in the material class of bladder wall, which can be used as the basis for development of structure-based constitutive models for urinary bladder wall tissue. Finally, the findings of extracellular matrix protein analyses demonstrated that changes in matrix protein contents of bladder tissue played significant role in bladder functional behavior, and suggested that elastin/collagen ratio might be the key factor in determining the compliance of bladder wall.

TABLE OF CONTENTS

| | | |
|---------|------------------------------------------------------------|----|
| 1.0 | INTRODUCTION | 1 |
| 1.1 | THE URINARY BLADDER..... | 2 |
| 1.1.1 | Anatomy of the Urinary Bladder | 2 |
| 1.1.2 | Histomorphology of the Urinary Bladder | 4 |
| 1.1.3 | Composition of the Detrusor..... | 7 |
| 1.1.3.1 | Smooth muscle cells | 7 |
| 1.1.3.2 | Extracellular matrix | 7 |
| 1.1.4 | Development of the Urinary Bladder..... | 10 |
| 1.1.4.1 | Collagen formation | 10 |
| 1.1.4.2 | Elastin formation..... | 11 |
| 1.1.5 | Physiology and Function of the Urinary Bladder | 13 |
| 1.1.5.1 | Micturition reflex | 13 |
| 1.1.5.2 | Neurosensory regulation..... | 14 |
| 1.2 | SPINAL CORD INJURY | 17 |
| 1.2.1 | Definition, incidence and prevalence..... | 17 |
| 1.2.2 | Complications associated with SCI | 17 |
| 1.2.3 | The effects of Spinal Cord Injury on Urinary Bladder | 18 |

| | | |
|-------|-----------------------------------------------------------------------------|----|
| 2.0 | REVIEW OF PREVIOUS STUDIES..... | 21 |
| 2.1 | FUNCTIONAL AND MECHANICAL PROPERTIES..... | 21 |
| 2.1.1 | Current Clinical Functional Evaluation: Cystometry and Urodynamics..... | 22 |
| 2.1.2 | Intact Organ Testing <i>in vitro</i> | 25 |
| 2.1.3 | Uniaxial Testing..... | 26 |
| 2.1.4 | Biaxial Mechanical Testing..... | 28 |
| 2.2 | STRUCTURE AND MORPHOLOGY OF THE BLADDER WALL IN SCI..... | 32 |
| 2.2.1 | Bladder enlargement and muscular hypertrophy..... | 32 |
| 2.2.2 | Area fraction and orientation of smooth muscle bundles in SCI bladders..... | 34 |
| 2.2.3 | Changes in collagen content..... | 38 |
| 2.2.4 | Changes in elastin content..... | 40 |
| 2.3 | SUMMARY OF CHANGES IN BLADDER TISSUE 10 DAYS AFTER SCI..... | 41 |
| 2.4 | HYPOTHESIS..... | 42 |
| 2.5 | OBJECTIVES..... | 43 |
| 2.5.1 | Extension of timeframe to 10 weeks after injury..... | 43 |
| 2.5.2 | Planar biaxial mechanical testing..... | 43 |
| 2.5.3 | Histomorphometry..... | 44 |
| 2.5.4 | Extracellular matrix proteins analyses..... | 44 |
| 2.5.5 | The overall goals..... | 45 |
| 3.0 | METHODS..... | 46 |
| 3.1 | MECHANICAL CHARACTERIZATION..... | 46 |
| 3.1.1 | Specimen preparation..... | 46 |
| 3.1.2 | Biaxial mechanical testing..... | 49 |

| | | |
|-------|-------------------------------------------------------|----|
| 3.1.3 | Data Analysis | 51 |
| 3.1.4 | Response Function | 52 |
| 3.2 | HYSTOMORPHOMETRY | 54 |
| 3.2.1 | Specimen preparation..... | 54 |
| 3.2.2 | Imaging of Rat Bladder Histological Sections..... | 55 |
| 3.2.3 | Muscle Orientation..... | 56 |
| 3.2.4 | Tissue Composition | 57 |
| 3.3 | QUANTIFICATION OF EXTRACELLULAR MATRIX PROTEINS | 58 |
| 3.3.1 | Specimen preparation..... | 58 |
| 3.3.2 | Data analysis | 58 |
| 4.0 | RESULTS | 59 |
| 4.1 | MECHANICAL TESTING | 59 |
| 4.1.1 | Stress-stretch response | 59 |
| 4.1.2 | Changes in the areal strain | 59 |
| 4.1.3 | Changes in the maximum axial stretches..... | 60 |
| 4.1.4 | Response function analysis..... | 61 |
| 4.2 | HISTOMORPHOMETRY STUDY | 63 |
| 4.2.1 | Smooth Muscle Orientation | 63 |
| 4.2.2 | Tissue Composition | 64 |
| 4.3 | ANALYSIS OF MATRIX PROTEIN CONTENTS | 65 |
| 4.4 | SUMMARY OF FINDINGS IN 10-WEEK SCI BLADDER..... | 67 |
| 5.0 | DISCUSSION..... | 68 |
| 5.1 | BIOMECHANICAL ANALYSES..... | 68 |

| | | |
|---------|-----------------------------------------------------------------------------|----|
| 5.1.1 | Changes in biomechanical properties of bladder wall | 68 |
| 5.1.2 | Bladder wall model prediction..... | 69 |
| 5.1.3 | Tissue structural information and its relation to mechanical behavior | 70 |
| 5.2 | MATRIX PROTEINS ANALYSIS..... | 72 |
| 6.0 | SUMMARY AND CONCLUSIONS | 75 |
| 6.1 | CHANGES IN THE MECHANICAL PROPERTIES | 75 |
| 6.2 | CHANGES IN THE BLADDER WALL COMPOSITION AND STRUCTURE..... | 76 |
| 6.3 | CONCLUSIONS..... | 77 |
| 6.4 | FUTURE STUDIES..... | 79 |
| 6.4.1 | Extended biochemical studies..... | 79 |
| 6.4.1.1 | The role of cross-linking..... | 79 |
| 6.4.1.2 | The role of actin and myosin | 80 |
| 6.4.1.3 | Collagen typing..... | 80 |
| 6.4.2 | Diversion Studies..... | 81 |
| 6.4.3 | Active Properties..... | 81 |
| 6.4.4 | Morphology studies | 82 |
| 6.4.5 | Advanced Modeling..... | 82 |
| | BIBLIOGRAPHY..... | 83 |

LIST OF TABLES

| | |
|----------------------------------------------------------------------------------------------------------------------------------------------------------------------------------------------------------------------------------------------------------------|----|
| Table 1: General effects of spinal cord injury on the urinary bladder function [2, 8, 40-43]..... | 19 |
| Table 2: Protocol for all specimens. See Figure 21 for graphical representation. | 50 |
| Table 3: Specimen weights, and collagen and elastin contents in the normal and SCI rat bladders (data are mean \pm SEM; *p<0.05; n=6-12; analyzed by one-way ANOVA followed by the Student-Newman-Keuls post-hoc test). † from [60]..... | 65 |
| Table 4: Collagen and elastin concentrations, and elastin/collagen ratios in the normal and SCI rat bladders (data are mean \pm SEM; *p<0.05; n=6-12; analyzed by one-way ANOVA followed by the Student-Newman-Keuls post-hoc test). † from [60]..... | 66 |

LIST OF FIGURES

- Figure 1:** Anatomical relationships between bladder and adjacent organs in female and male. ... 2
- Figure 2:** Frontal cross-section schematic of a human urinary bladder as in female (upper left) and male (lower right). Reproduced from Netter, Atlas of Human Physiology, 1997. 3
- Figure 3:** Histology of the normal rat bladder wall, stained with Movat Pentachrome technique, 40X. Urothelium (A), lamina propria (B), and detrusor (C)..... 4
- Figure 4:** Schematic of bladder layers and constituent components. The scale of the components is approximately correct for normal bladder wall [17]. 6
- Figure 5:** Collagen bundles (stained in yellow) located between smooth muscle fascicles in normal rat bladder wall, stained with Movat Pentachrome technique, 40X..... 9
- Figure 6:** Schematic of electrical pathways that operate as part of the micturition reflex, demonstrating interaction between regulatory/sensory and reflex loops (A), and possible sites of breakdown in the neurosensory pathways and the consequent results (B). (Retrieved from www.life-tech.com/uro/urolib/normant.htm, July 2005) 14
- Figure 7:** Sympathetic, parasympathetic, and somatic innervation of the urogenital tract of the male cat. Sympathetic preganglionic pathways emerge from the lumbar spinal cord and pass to the sympathetic chain ganglia (SCG) and then via the inferior splanchnic nerves (ISN) to the inferior mesenteric ganglia (IMG). Preganglionic and postganglionic sympathetic axons then travel in the hypogastric nerve (HGN) to the pelvic plexus and the urogenital organs. Parasympathetic preganglionic axons, which originate in the sacral spinal cord, pass in the pelvic nerve to ganglion cells in the pelvic plexus and to distal ganglia in the organs. Sacral somatic pathways are contained in the pudendal nerve, which provides an innervation to the penis, and the ischiocavernosus (IC), bulbocavernosus (BC), and external urethral sphincter (EUS) muscles. The pudendal and pelvic nerves also receive postganglionic axons from the caudal sympathetic chain ganglia. These three sets of nerves contain afferent axons from the lumbosacral dorsal root ganglia. PG = prostate gland; U = ureter; VD = vas deferens (Redrawn from [2])..... 15
- Figure 8:** The overall current concept of bladder biomechanical function..... 22
- Figure 9:** An example of combined cystometrograms and sphincter electromyograms (EMGs) comparing reflex voiding responses in an infant (A) and in a paraplegic patient (C) with a voluntary voiding response in an adult (B). The abscissa in all records represents bladder

volume in milliliters, and the ordinate represents bladder pressure in cm H₂O and electrical activity of the EMG recording. On the left side of each tracing, the arrows indicate the start of a slow infusion of fluid into the bladder (bladder filling). Vertical dashed lines indicate the start of sphincter relaxation, which precedes by a few seconds the bladder contraction in A and B. In B, note that a voluntary cessation of voiding (stop) is associated with an initial increase in sphincter EMG followed by a reciprocal relaxation of the bladder. A resumption of voiding is again associated with sphincter relaxation and a delayed increase in bladder pressure. In the paraplegic patient (C), the reciprocal relationship between bladder and sphincter is abolished. During bladder filling, transient uninhibited bladder contractions occur in association with sphincter activity. Further filling leads to more prolonged and simultaneous contractions of the bladder and sphincter (bladder-sphincter dyssynergia). Loss of the reciprocal relationship between bladder and sphincter in paraplegic patients interferes with bladder emptying (Redrawn from [2])...... 24

Figure 10: Representative response of isolated strips of fetal and adult calf bladder to field stimulation (64 Hz) following bethanechol prestimulation (200 μM) in a uniaxial testing. Arrows indicate initiation of field stimulation (Redrawn from [74]). 27

Figure 11: The reduced relaxation function G(t) applied to stress relaxation data of normal and SCI bladders for a peak biaxial stress of (a) 25 kPa and (b) 100 kPa. The model fitted the data for both groups successfully ($R^2 > 0.98$). (c) Schematic representation of the bladder as composite structures under stress relaxation. Compared to the normal rat bladders, SCI rat bladders contained more smooth muscle and elastin, but similar amounts of collagen. As a result, SCI bladders exhibited increased distensibility and decreased rate of stress relaxation. This is due to different viscoelastic behaviors of smooth muscle, collagen, and elastin, which exhibits large, medium, and virtually no stress relaxation, respectively (Redrawn from [60]). 31

Figure 12: Photomicrographs of histological slides of the normal (A) and 10-day SCI (B) rat bladders, stained with Movat Pentachrome technique, mag. 10X. Both structural layers of bladder wall, lamina propria and detrusor, are significantly thicker in SCI sample when compare to the normal (Redrawn from [60]). 33

Figure 13: Area fractions of muscle and collagen in normal and 10-day SCI rat bladders at different volume levels. The SCI bladders exhibited significant (* $p < 0.05$) increases in smooth muscle and decreases in collagen area fractions compared to the normal bladders at all the volume levels examined. Data are mean ± SD; n= 5; analyzed by Two-way ANOVA followed by the Student-Newman-Keuls post-hoc test (Redrawn from [81]). 34

Figure 14: Nuclei counts of smooth muscle cells in normal and 10-day SCI rat bladders at different volume levels. The SCI bladders (black columns) exhibited significantly (* $p < 0.001$) fewer cell nuclei per muscle area compared to the normal bladders (white columns). Data are mean ± SD; n= 15; analyzed by Two-way ANOVA followed by the Student-Newman-Keuls post-hoc test. † The values are normalized by the area fractions of muscle (Redrawn from [81]). 35

| | |
|-----------------------------------------------------------------------------------------------------------------------------------------------------------------------------------------------------------------------------------------------------------------------------------------------------------------------------------------------------------------------------------------------------------------------------------------------------------------------------------------------------------------------------------------------------------------------------------------------------------------------------------------------------------------------|----|
| Figure 15: The orientation distribution of muscle bundles in normal and SCI rat bladders. In the normal bladders (A) the predominant muscle orientation was along the longitudinal axis, while the 10-day SCI bladders (B) had predominant muscle orientation along both longitudinal and circumferential axes at all volume levels examined (25%, 50%, ∇ 100%). Colored triangles represent longitudinal (blue) and circumferential (red) biases (Redrawn from [81]). | 37 |
| Figure 16: Photomicrographs of human detrusor bladder tissue from control (A), idiopathic (B), and neuropathic bladders (C). Normal areas are signified by *, and † indicates a severely affected area in B. The scale bar is 200 μm [17]. | 39 |
| Figure 17: Digital images of a histology slide of 10-day SCI rat bladder, stained with Movat Pentachrome technique, mag. 40X. Increased amount of elastic fibers (stained in black; indicated by arrows) is notable (Redrawn from [60]). | 40 |
| Figure 18: The altered mechanical environment of the urinary bladder following spinal cord injury, the key signal for the changes in the tissue functional properties. | 42 |
| Figure 19: Rat bladders were cut open longitudinally along the urachus (panel A). Graphite makers were attached on the luminal surface (panel B). The test specimen was mounted on the biaxial testing device using stainless steel hooks and nylon suture lines (panel C). | 48 |
| Figure 20: Image of sample attached to biaxial testing device through stainless steel hooks and nylon suture lines. | 49 |
| Figure 21: Stress-controlled biaxial mechanical protocols. | 50 |
| Figure 22: Mapping of the real-time positions of four tissue markers from the reference configuration to the deformed configuration, allowing for bi-linear interpolation of the displacement field (Redrawn from [76]). | 51 |
| Figure 23: Schematic representation of the bladder histology specimen preparation. (a) The rat bladders were fixed in formalin under the filled condition at various volume % (25%, 50%, and 100%) overnight and cut open longitudinally along the urachus on the anterior (ventral) side; (b) a rectangular section was cut from the posterior (dorsal) side directly opposite of the initial cut; (c) a uniform size (5mm × 8mm) sections were embedded in paraffin; and (d) each piece was sectioned en face (approximately 5μmthick) throughout the thickness of the bladder wall and stained using the Movat’s Pentachrome technique (Redrawn from [81]). | 55 |
| Figure 24: (A) Schematic showing the regions on the tissue section where the images were taken from (Redrawn from [81]); (B) Example image of a 10-week SCI bladder section, stained with Movat Pentachrome technique, mag. 10X. | 56 |
| Figure 25: Representative stress-strain response to protocols listed in Table 3-2 for one normal specimen. | 59 |

Figure 26: Changes in the mechanical compliance of the bladder wall up to 10 weeks after SCI. Areal strain, as an index of tissue compliance, was calculated (data are mean \pm SEM) in 3-week, 6-week and 10-week SCI specimens (* $p < 0.05$, $n = 6-12$, analyzed by ANOVA followed by Dunn's post-hoc test; † redrawn from [58], § redrawn from [17]). 60

Figure 27: Biaxial mechanical response in the bladder specimens. Maximum axial stretches were determined in circumferential and longitudinal directions in normal and 1.5-, 3-, 6-, and 10-week SCI rat bladders (data are mean \pm SEM; * $p < 0.05$; $n = 6-12$; analyzed by ANOVA followed by a post hoc test; § redrawn from [17]). 61

Figure 28: Stress contours for normal, 10-day SCI (redrawn from [17]), and 10-week SCI rat bladder wall, along with the actual strain values. Left column is designated to S_{11} and right column is for S_{22} . Solid diagonal lines are the $E_{11} = E_{22}$ identity, which is shown for visual reference. 62

Figure 29: The orientation distribution of muscle bundles in 10-week SCI rat bladders, fixed at 50% volume capacity, $n = 3$ 63

Figure 30: Area fractions of muscle and collagen in normal, 10-day and 10-week SCI rat bladders, fixed at 50% volume capacity. The 10-week SCI bladders exhibited significant (* $p < 0.05$) increases in collagen area fractions compared to the 10-day SCI group, but similar to the normal bladders. Data are mean \pm SD; $n = 3-5$; analyzed by One-way ANOVA followed by the Student-Newman-Keuls post-hoc test. † Redrawn from [81]. 64

Figure 31: Comparison between results of mechanical testing and histomorphometry study. Upper panel: The longitudinal (\circ) and circumferential (\bullet) stress-stretch curves representing equibiaxial data (mean \pm SEM) in normal and SCI rat bladders indicated an isotropic response in 1.5-week SCI samples [17], but an anisotropic behavior in normal and 10-week SCI bladders. Lower panel: The orientation distribution of muscle bundles in normal (A), 1.5-week SCI (B) (redrawn from [81]), and 10-week SCI (C) bladders corroborated the mechanical anisotropy data. 71

Figure 32: Digital image of histology slide 10-week SCI rat bladder, stained with Movat Pentachrome technique, mag. 40X. Increased amount of elastic fibers (stained in black; indicated by arrows) is notable. 73

Figure 33: The changes in areal strain and elastin/collagen concentration ratio in rat bladder tissue over a period of 10 week after injury (those of normal bladder shown at zero time point). The similarity of two plots as a function of time suggests a potential correlation between them. 74

Figure 34: Areal strain at various time-points after injury plotted as a function of corresponding elastin/collagen ratio, exhibiting a linear correlation between them. 74

PREFACE

First and foremost, I would like to thank my wonderful wife, Marjan. My graduate work would not be complete without constant encouragement and support from her, as well as from her mom, who has been no less than a mother to me too. Special thanks to my in-laws, Behrooz for his unlimited supply of delicious pizza and for taking me to the soccer games, Ben for his generosity, and Mojgan for her love and support. I would also like to thank my son, Nicholas, for making my life more meaningful. I dedicate my thesis to him, because he was the sole reason and main motivation for me to go back to school at age 32. Thanks also to my parents and my sister for constantly reminding me about my past.

Thanks foremost to the National Institutes of Health for funding my graduate work through their Training Grant T32 DK07774 and the Program Project Center for Urologic Research Excellence-Spinal Cord Injury HD39768-01A1. Also special thanks to Paralyzed Veterans of America Spinal Cord Research Foundation for providing me with my educational costs and fees through Dr. Jiro Nagatomi's grant (#2289-01).

So many thanks to the Department of Bioengineering. My very special thanks to Professor Harvey Borovetz for being the best Department Chair in the whole world, not only for what he has done for me and other Pitt bioengineering students, but also for the way he has been doing it: wisely, respectfully and always with a smile. Thanks very much to Lynette Spataro, Joan Williamson, Billie Bergman and Kristie Moran for always helping me through my academic problems, which have often been very unorthodox.

I would like to thank many of the past and present students and staff of the Engineered Tissue Mechanics Laboratory (ETML). Many thanks to Ali Mirnajafi, Ph.D. for introducing me to the ETML. My very special thanks to Claire Gloeckner, Ph.D. for her wonderful work on the

urinary bladder, which provided me with a great foundation for my research projects. Thanks David Merryman for making ETML a better place to work. Thanks Brett Zubiante for his support when we had technical problems. Also, my appreciation to Todd Courtney for his excellent skills in programming, and to Jonathan Grashow for his outstanding talents and creativity, which without them I would have more difficulties to complete my research projects. Many thanks to Rebecca Long, John Stella and Ajay Abad for being there when I was in need. Also special thanks to Silvia Wognum, not only for helping me while I was completing my thesis, but also for continuing the work on the bladder research projects. I would like to wish good luck to her and other ETML new students, Erinn Joyce, Chad Eckert, and Diana Gaitan toward their doctoral work. My thanks to Anna Goldman for being a great mother-figure for all of us in ETML. God bless her.

I would like to thank the people at the CURE-SCI lab in the Department of Urology, directed by Naoki Yoshimura, M.D., Ph.D. Many thanks to Fernando De Miguel, Ph.D. and Vickie Erickson for helping me with my research needs. Special thanks to many people in the Urology lab for obtaining rat bladder specimens for me, including Drs. Kazumasa Torimoto, Teruyaki Ogawa, Cathy Thomas, Masataka Yano, Yukio Kansei and Rachelle Prantil.

My everlasting gratitude to my graduate committee members, Michael Chancellor, M.D., for his great vision and distinguished leadership, and Jiro Nagatomi, Ph.D. for walking me through the world of research, being my mentor, friend, and co-advisor. Last, but definitely not least, I would like to thank my advisor Professor Michael Sacks for giving me the unique opportunity to rebuild my career life. I appreciate all the valuable time and training and also the financial support he has given me as his graduate student. I have learned a lot from him, even more than he intended to teach me, and just because of that I will eternally be grateful.

1.0 INTRODUCTION

Approximately 250,000 – 400,000 individuals in the United States have spinal cord injuries (SCI); urologic complications are among the most common problems these patients encounter [1]. Specifically, spinal cord injuries rostral to the lumbar spine can cause severe lower urinary tract dysfunctions including overactive bladders and urinary retention [2]. These bladder abnormalities are reportedly accompanied not only by changes in the bladder wall tissue morphology, including increased thickness [3], fibrosis [4] and trabeculation [5], but also by drastic changes in the mechanical properties of the wall [6, 7]. Although extensive studies have been conducted on the effects of spinal cord injury on bladder function [8-11], the alterations in mechanical behavior and functional properties of the bladder wall tissue and the underlying mechanisms are not well understood. In order to gain a better understanding of relationship between function and structure of bladder wall following SCI, the present study combined different experimental methods (including mechanical testing, biochemical assays and histomorphometry) to investigate changes in mechanical properties, as well as alterations in composition and morphology of the bladder wall tissue at various time points up to 10 weeks after injury.

1.1 THE URINARY BLADDER

1.1.1 Anatomy of the Urinary Bladder

The bladder is a hollow organ in the pelvis that stores the urine produced by the kidneys. There are two tubular structures called ureters (one from each kidney) that drain the urine into the bladder. The urethra is the outflow tract of the bladder and connects the bladder to the exterior (Figure 2).

Anatomically, bladder is the most anterior organ in the pelvis, located just behind the pelvic bone. Organs closest to the bladder include the rectum (the last part of the colon), which is the most posterior organ in the pelvis, the prostate gland and seminal vesicles (in males), and the uterus, ovaries and fallopian tubes (in females). In males, the prostate gland and seminal vesicles (organs that contribute secretions in semen) are situated below the bladder and in front of the rectum. In females, the uterus (the womb), ovaries and fallopian tubes are located posterior the bladder and anterior to the rectum (Figure 1).

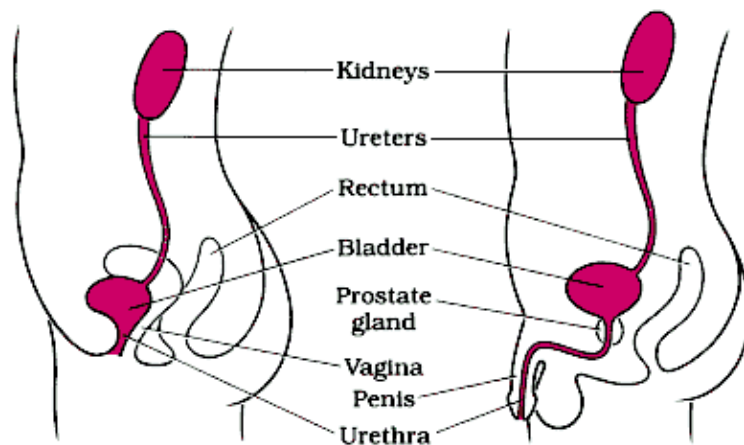


Figure 1: Anatomical relationships between bladder and adjacent organs in female and male.

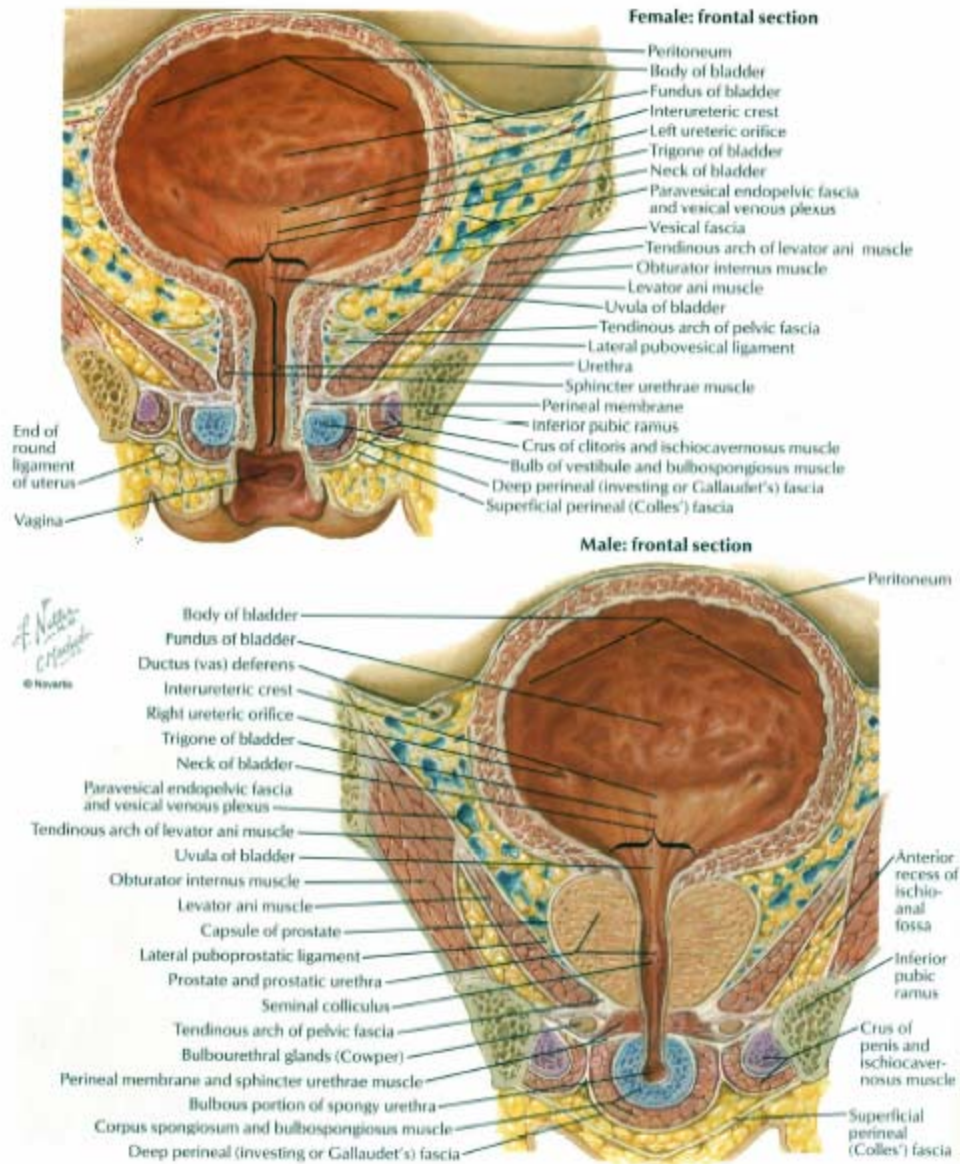


Figure 2: Frontal cross-section schematic of a human urinary bladder as in female (upper left) and male (lower right). Reproduced from Netter, Atlas of Human Physiology, 1997.

1.1.2 Histomorphology of the Urinary Bladder

The urinary bladder consists of two major layers, each comprised of several sublayers: the lamina propria near the lumen and the muscularis propria (*i.e.* the detrusor) on the exterior of the bladder (Figure 3) [12]. A healthy human bladder contains a lamina propria that is approximately 1.3 mm thick and a detrusor layer about 4.4 mm thick [4].

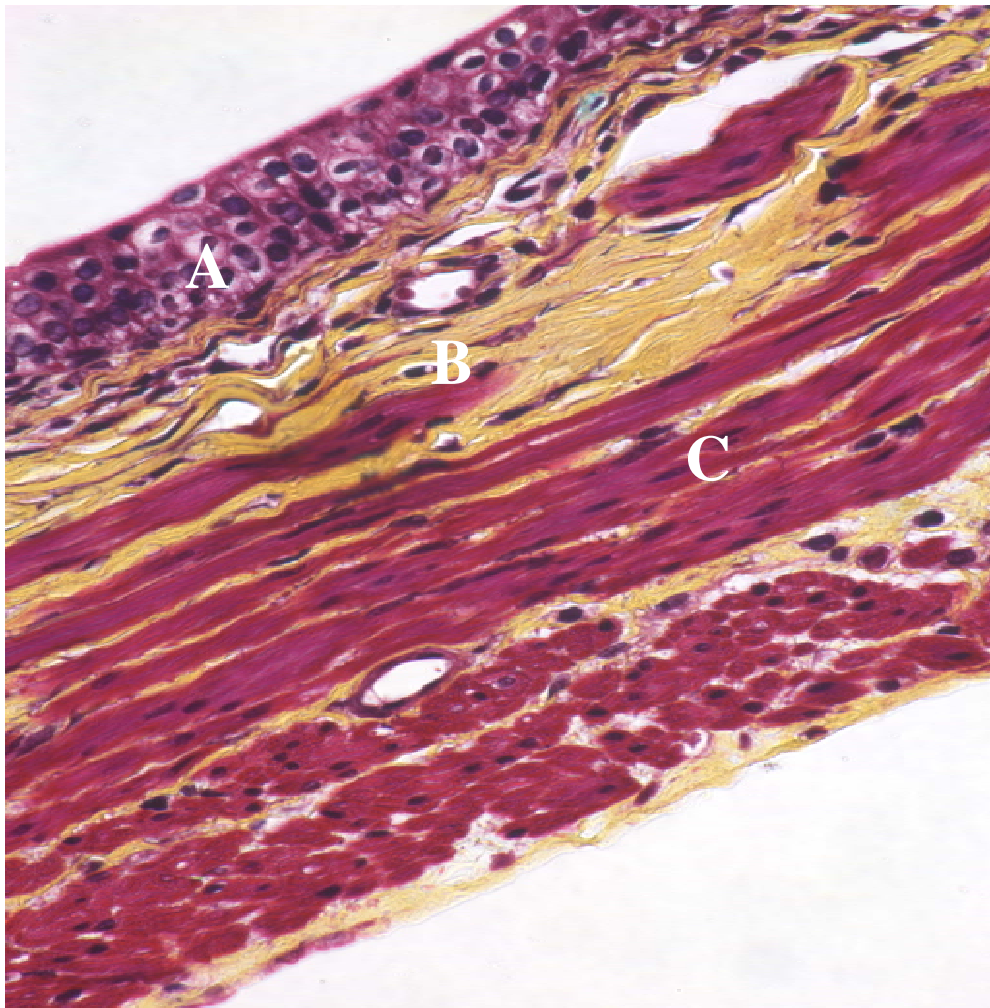


Figure 3: Histology of the normal rat bladder wall, stained with Movat Pentachrome technique, 40X. Urothelium (A), lamina propria (B), and detrusor (C).

a. Lamina propria

The lamina propria is composed of the urothelium, the superficial lamina propria, and the deep layers of the lamina propria (Figure 4).

i. Urothelium

The epithelium, which lines the bladder and is in contact with the urine, is referred as transitional epithelium or urothelium. The urethra, ureters and the pelvis of the kidney are also lined by this urothelium. The normal urothelium is several cell layers thick and is composed of umbrella cells. These cells provide the barrier that isolates the toxic urine from the bloodstream and the rest of the body.

ii. Superficial lamina propria

Directly beneath the urothelium is a layer of connective tissue and blood vessels (*i.e.* the capillary network of the bladder) called the superficial portion of the lamina propria [13, 14]. This layer is a dense weave of randomly oriented collagen fibers [13]. Within the superficial lamina propria, there is a thin and often discontinuous layer of smooth muscle called the muscularis mucosae. This superficial layer of smooth muscle is not to be confused with the true muscular layer of the bladder called the muscularis propria or detrusor muscle.

iii. The deeper lamina propria

A thick layer of collagen (more than 300 μm in the human adult) [13], maintains the shape of the bladder wall.

b. Muscularis propria or detrusor muscle

The next layer from the lumen is the muscular detrusor of the bladder. This deep muscle layer consists of thick smooth muscle bundles that form the wall of the bladder and contract during emptying. The major smooth muscle layer of the detrusor is composed of muscle bundles or

fascicles (groups of muscle cells) of diameter 50 to 150 μm in various orientations. The detrusor layer also contains fibroblast-like cells that, along with the smooth muscle cells, secrete proteins that make up the connective tissue matrix that surrounds and lies within the smooth muscle fascicles [15]. Finally, the outer serosal or adventitial layer covering the external surface of the bladder is a dense layer of fine collagen fibrils of diameter 1-3 μm and about ten microns thick [4, 13]. In addition, a network of nerves including myelinated fibers, is found in all layers of the bladder and these nerves are sheathed in connective tissue [16].

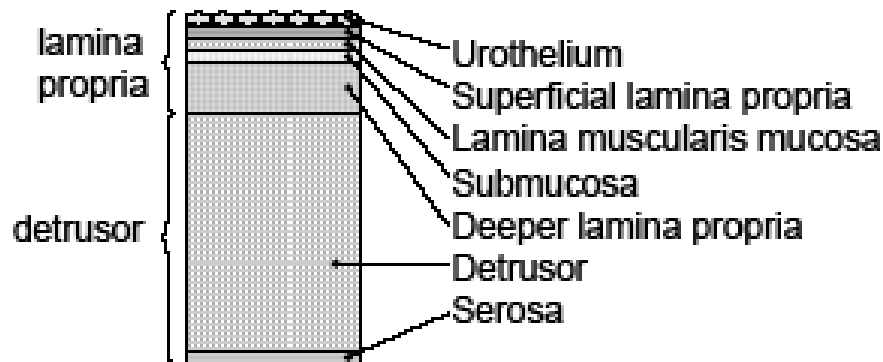


Figure 4: Schematic of bladder layers and constituent components. The scale of the components is approximately correct for normal bladder wall [17].

1.1.3 Composition of the Detrusor

The major components of the urinary bladder wall are smooth muscle cells and the extracellular matrix (ECM).

1.1.3.1 Smooth muscle cells

Within the detrusor layer, the smooth muscle fascicles are 20-50 μm apart [13]. The majority of them are directional in certain areas of the bladder. These fascicles are interconnected with collagen bundles of diameter 3 to 8 μm in the rat [13]. Significant amounts of perimysial connective tissue connects the muscle fascicles (Figure 5), and minimal endomysial connective tissue matrix surrounds individual muscle cells [4].) There are also small elastic fibers between muscle cells within fascicles [16].

1.1.3.2 Extracellular matrix

Extracellular matrix in the bladder wall tissue is mainly composed of two protein components, collagen and elastic fibers.

I. Collagen

The human urinary bladder is approximately 30-60% collagen dry weight [18, 19]. This percentage content depends on the age and health of the bladder; collagen content tends to increase with development and may change in the presence of disease. In human fetal bladders, the percentage is near 30% [19], while in human adults, it is 53% - 68%, with higher percentages in women over fifty years of age [20]. In addition, the trigone, or base, has a higher percentage of collagen than the body and dome of the bladder [20].

Types I, III, VI, and V collagen are the major collagen components of the bladder, with type I the most plentiful [21]. Types I and III together make up 80-99% of total collagen in the body [22] and more than 98% of the collagen in the bladder, as heterotypic fibrils [20, 21]. In children, normal bladders contain 76.3% type I and 23.8% type III collagen [12, 23].

In a study of human bladder, Kim and colleagues found that thick collagen fibers, classified as type I collagen, were predominant in the intermuscular bundle space; thin collagen fibers (type III collagen) were abundant between individual muscle cells within the muscle fascicles [19]. Type III has also been found coating the exterior of fascicles [24] and connecting neighboring fascicles in cattle and rats [13, 20]. Both types I and III are coiled structures within detrusor and associated with perimysial connective tissue around muscle fascicles [25]. Type III collagen also exists in a coiled configuration in the urinary bladder to allow for large strains [12, 14, 20].

The other types of collagens contribute only 1-2 % of the total dry weight collagen in the bladder. Type IV forms a cocoon-like sheath that surrounds each individual smooth muscle cell in the bladder wall [20]. Collagen types XII and XIV connect collagen fibrils to other extracellular matrix components associated with the surface of fibrillar collagens, and may mediate interaction between collagen fibrils and extracellular matrix proteins or the cell surface [26]. Type XII collagen has been found in the lamina propria and in the endomysium in the detrusor [26]. Type XIV collagen has been found in the submucosa and in the serosa as well as in the perimysial tissues between the smooth muscle fascicles in small amounts in rats [26]. Other collagen types are present in negligible amounts.

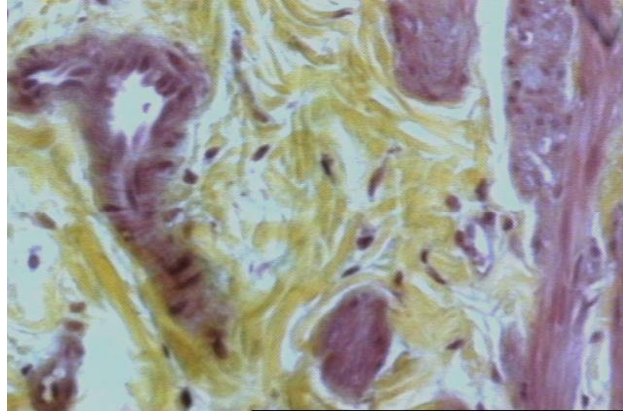


Figure 5: Collagen bundles (stained in yellow) located between smooth muscle fascicles in normal rat bladder wall, stained with Movat Pentachrome technique, 40X.

II. Elastin

It has been shown that elasticity of the bladder, like other organs subjected to repeated deformation, is inherent in elastic fibers [18]. In other words, the ability of the bladder to maintain the low filling pressures that prevent permanent upper tract deterioration may depend on the elastic component of the bladder wall [27]. Although the structure of elastin is less understood than that of collagen, the elastic fibers are thought to be composed of several glycoproteins [28]. In the urinary bladder, elastin has been found in the urothelium layer and adjoining lamina propria [29], around individual smooth muscle cells [30, 31], within the connective tissue connecting the fascicles [29], in the interfascicular space, and in the outermost layer of the serosa [31].

1.1.4 Development of the Urinary Bladder

During gestation, the fetal kidneys and bladder remove toxin from the blood. During the earliest stage of gestation, fetal urine is not emptied through the urethra but instead through the urachus, a soft tissue tube emanating from the dorsal part of the dome of the bladder. Fetal urine leaves the developing fetus through the umbilical cord. The urachus contains smooth muscle; experiments in fetal sheep have demonstrated muscle tone and contraction within it [30]. In the bovine and ovine species, the urachus closes off just before birth, while in humans this happens at about 4 months into gestation. It is likely that the closing of the urachus, which requires the bladder to start functioning as a storage vessel, may trigger the final development [30].

In cattle, bladder wall thickness increases throughout the development period into adulthood; however, the total dry weight of collagen does not change after the second trimester of gestation [32]. Cystometrograms measuring the bovine bladder compliance (pressure to volume ratio) demonstrate an increase in the maximum volume during development followed by a decrease during early adulthood [32-34]. This increase and then decrease in bladder compliance indicate concomitant changes in structural makeup. In addition, it has been discovered that the removal of the detrusor layer of the bladder results in increased compliance throughout fetal developmental, but compliance increases most in the second trimester and least in the third trimester [33].

1.1.4.1 Collagen formation

Throughout the development in the human, the total collagen-to-smooth-muscle ratio decreased from 1.1 to 0.65, indicating more smooth muscle cell growth than deposition of collagen [19]. The expression of the mRNA of the two chains composing collagen type I, $\alpha 1(I)$ and $\alpha 2(I)$, was

higher during bovine fetal gestation by three to six times compared with the adult state [30]. In the second trimester, type I collagen was localized to the lamina propria while in the third trimester the localization of type I collagen was plentiful within the central region of the lamina propria [30]. The peak expression of type I during the early third trimester was an indication that the bladder was strengthening since this was when the bladder first began to function properly at low pressure and empty completely because the urachus has closed [30].

Type III collagen predominated in newly formed fetal structures, including the bladder and in early wound healing, so it is often called fetal or embryonic collagen [30]. At the earliest stages of bovine gestation, the amount of collagen type III was high in the fetal bladder, composing up to 40% of the collagen in the bladder; by birth, it dropped to 19%. It increased slightly during growth and development to 25% in the adult animal [32].

The levels of $\alpha 1(\text{III})$ mRNA in a whole bladder preparation peaked in the youngest bovine gestational stages in the detrusor of the bladder and gradually declined throughout gestation [21, 25]. In the second trimester, type III collagen was localized to the lamina propria and around the muscle fascicles [25]. Changes in the collagen I: collagen III ratio differed between studies. For example, one study showed that the absolute amount of type III collagen decreased by greater than half from the beginning of the second trimester to newborn in the calf [20, 32], yet human and bovine studies have demonstrated a decrease in the ratio through gestation [19, 20].

1.1.4.2 Elastin formation

Three known elastic fiber related proteins (elastin, fibrillin-1, and MAGP) found throughout all bovine developmental stages [30]. Levels of fibrillin-1 and MAGP were higher in the fetal period compared to postnatal [30]. In the human, the size, thickness, and number of elastic fibers

increased during human gestation as the organ developed [19]. Elastin mRNA levels were highest in the second trimester, the earliest stage measured, and decreased until birth [30]. In both the second and third trimesters, fibrillin-1 and MAGP localized to the fine fibers in the lamina propria and the basal cells of the urothelium, and elastin was found in similar locations but in lower concentrations [30]. In the third trimester and at term, all three proteins measured localized to the lamina propria [30]. Elastin levels increased through gestation and higher levels were found in the third trimester, but there was decreased expression in the calf at full term [29]. The peak of microfibrillar mRNA occurred in the early third trimester, coinciding with peak expression of type I collagen [30]. After birth there was no change in the detrusor layer elastin expression but an increase in the urothelial-lamina propria layer in both young and adult animals, similar to type III collagen, which is highest early in development and then decreases as the fetus matures [30]. It is possible that steady-state mRNA levels of elastin in post-natal bladders are related to the requirement for increased bladder volume as the animal grows [30]. The accumulation of elastin declines rapidly by end of first year followed by little or no new production after the first decade. Also, the turnover rates of insoluble elastin are very low, with half-life protein measurements ranging in years [35].

It has been postulated that the mechanical properties of the bladder wall are primarily bestowed by the extracellular matrix components [19, 36]. In particular, collagen is thought to provide tensile strength, whereas elastic fibers are thought to enhance tissue elasticity. Kim *et al* [19] demonstrated that a delicate balance in their production is responsible for the development of normal urinary bladder function during fetal growth. In addition to playing a role in neonatal bladder dysfunction, changes in extracellular matrix may play a role in the bladder dysfunction

associated with pathological conditions in the adult. It is, therefore, important in any study of alterations in pathological tissues to quantify and/or evaluate the changes in these proteins.

1.1.5 Physiology and Function of the Urinary Bladder

Urinary bladder is a muscular sac that stores urine at low pressure, and voids upon receiving neural inputs to contract the smooth muscle. Urine enters the bladder from the kidneys through the ureters and is discharged from the body via the urethra. The bladder of the adult human can hold over 0.6 liters of urine. When the level of urine reaches about half this amount, pressure of the accumulating fluid stimulates nervous impulses that relax the external sphincter, a muscle that forms a dense band around the urethra at the base of the bladder. The muscles in the wall of the bladder also contract simultaneously, forcing urine out through the urethra. This process can be controlled voluntarily in most mammals [2].

1.1.5.1 Micturition reflex

The micturition reflex is a two-phase cycle that serves as a protective mechanism for the kidneys. It consists of the filling (or storage) phase and the emptying phase. This reflex is uninhibited in the newborns, and the toddlers will learn to inhibit (or control) it as they grow up. The ability to control the micturition reflex is dependent upon two systems being intact. These systems are (1) receptors and chemicals that must maintain a delicate balance for the muscles to operate properly, and (2) a neuro/sensory pathway that must be intact between the brain, spinal cord and bladder, so that the receptors can elicit an appropriate response. Receptors in the bladder communicate with receptors in the brain, via the spinal cord, to control the micturition reflex [2].

1.1.5.2 Neurosensory regulation

There are two electrical pathways that operate as part of the micturition reflex. These are the reflex loop and the regulatory/sensory loop (Figure 6).

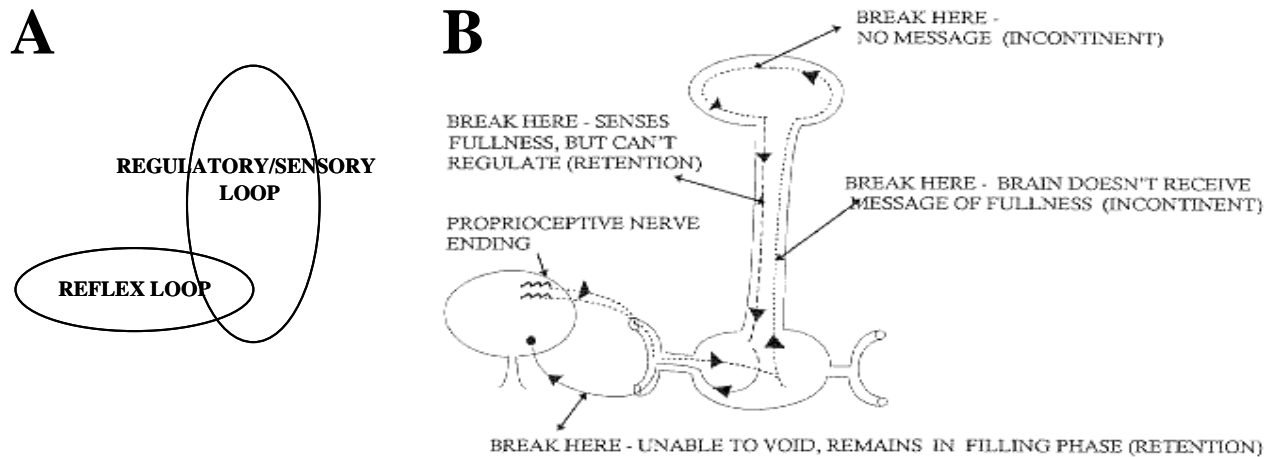


Figure 6: Schematic of electrical pathways that operate as part of the micturition reflex, demonstrating interaction between regulatory/sensory and reflex loops (A), and possible sites of breakdown in the neurosensory pathways and the consequent results (B). (Retrieved from www.life-tech.com/uro/urolib/normant.htm, July 2005)

The reflex loop is composed of three sets of peripheral nerves in the bladder and their connections to the spinal cord, including sacral parasympathetic (pelvic nerves), thoracolumbar sympathetic (hypogastric nerves and sympathetic chain), and sacral somatic nerves (pudendal nerves) (Figure 7). The main excitatory input to the bladder is provided by sacral parasympathetic outflow. Cholinergic preganglionic neurons located in the sacral spinal cord send axons via the pelvic nerves to ganglion cells in the pelvic plexus and in the wall of the bladder. Sympathetic preganglionic pathways that arise from the T₁₁ to L₂ spinal segments pass to the sympathetic chain ganglia and then to prevertebral ganglia in the superior hypogastric and pelvic plexuses and also to short adrenergic neurons in the bladder and urethra. Sympathetic

postganglionic nerves that release norepinephrine provide an excitatory input to smooth muscle of the urethra and bladder base, an inhibitory input to smooth muscle in the body of the bladder, and inhibitory (α_2) and facilitatory (α_1) input to vesical parasympathetic ganglia. Somatic efferent pathways to the external urethral sphincter are cholinergic and are carried in the pudendal nerve from anterior horn cells in the third and fourth sacral segments. Branches of the pudendal nerve and other sacral somatic nerves also carry efferent impulses to muscles of the pelvic floor [2].

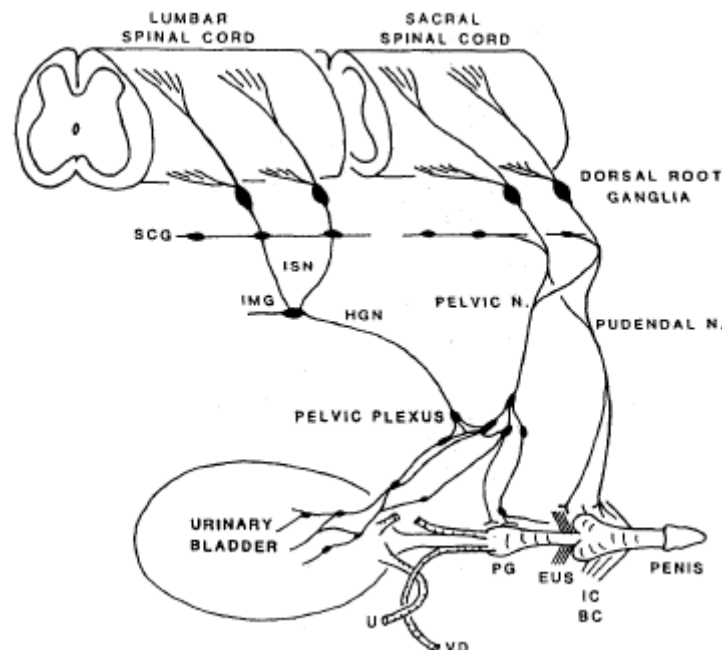


Figure 7: Sympathetic, parasympathetic, and somatic innervation of the urogenital tract of the male cat. Sympathetic preganglionic pathways emerge from the lumbar spinal cord and pass to the sympathetic chain ganglia (SCG) and then via the inferior splanchnic nerves (ISN) to the inferior mesenteric ganglia (IMG). Preganglionic and postganglionic sympathetic axons then travel in the hypogastric nerve (HGN) to the pelvic plexus and the urogenital organs. Parasympathetic preganglionic axons, which originate in the sacral spinal cord, pass in the pelvic nerve to ganglion cells in the pelvic plexus and to distal ganglia in the organs. Sacral somatic pathways are contained in the pudendal nerve, which provides an innervation to the penis, and the ischiocavernosus (IC), bulbocavernosus (BC), and external urethral sphincter (EUS) muscles. The pudendal and pelvic nerves also receive postganglionic axons from the caudal sympathetic chain ganglia. These three sets of nerves contain afferent axons from the lumbosacral dorsal root ganglia. PG = prostate gland; U = ureter; VD = vas deferens (Redrawn from [2])

The regulatory/sensory loop is composed of ascending sensory neurons in the spinal cord connected, through the motor cortex in the brain, to motor neurons in the regulatory tract of the spinal cord. In particular, this loop controlling micturition consists of four basic components: spinal efferent neurons, spinal interneurons, primary afferent neurons, and neurons in the brain that modulate spinal reflex pathways [2].

During bladder filling, the external and internal sphincters are contracted, due to somatic and sympathetic nerves activity, respectively. Sympathetic pathways inhibit detrusor activity facilitating urine storage. Sacral parasympathetic outflow is also inactive due to ganglionic inhibition by sympathetic nerves, which contributes to the maintenance of urinary continence. Intravesical pressure measurements during bladder filling in both humans and animals reveal low and relatively constant bladder pressures when bladder volume is below the threshold for inducing voiding [2].

Proprioceptive nerve endings in the bladder are stretched during the filling phase, and as approaching the micturition threshold, send information to the cortex that is perceived as fullness, discomfort, or pain [37]. The storage phase of the urinary bladder, then, can be switched to the voiding phase either involuntarily (*e.g.* in the human infant) or voluntarily. At this point, increased afferent firing from tension receptors in the bladder reverses the pattern of efferent outflow, producing firing in the sacral parasympathetic pathways and inhibition of sympathetic and somatic pathways. The expulsion phase consists of an initial relaxation of the urethral sphincter followed in a few seconds by a contraction of the bladder, an increase in bladder pressure, and flow of urine. There are also secondary reflexes elicited by flow of urine through the urethra facilitate bladder emptying [37]. All these pathways require the integrative action of neuronal populations at various levels of the neural axis [2].

1.2 SPINAL CORD INJURY

1.2.1 Definition, incidence and prevalence

Spinal Cord Injury (SCI) is damage to the spinal cord that results in a loss of function such as mobility or feeling. Frequent causes of damage are trauma (car accident, gunshot, falls, etc.) or disease (polio, spina bifida, Friedreich's Ataxia, etc.). The spinal cord does not have to be severed in order for a loss of functioning to occur. In fact, in most people with SCI, the spinal cord is intact, but the damage to it results in loss of functioning. SCI is very different from back injuries such as ruptured disks, spinal stenosis or pinched nerves.

It is estimated that the annual incidence of spinal cord injury (SCI), not including those who die at the scene of the accident, is approximately 40 cases per million population in the United States or approximately 11,000 new cases each year. Since there have not been any overall incidence studies of SCI in the U.S. since the 1970's it is not known if incidence has changed in recent years [38]. The number of people in the United States who are alive in July 2004 who have SCI has been estimated to be approximately 247,000 persons, with a range of 222,000 to 285,000 persons [38].

1.2.2 Complications associated with SCI

The effects of SCI depend on the type of injury and the level of the injury. SCI can be divided into two types of injury - complete and incomplete. A complete injury leads to loss of function, sensation and voluntary movement below the level of the injury. An incomplete injury may spare some functioning below the primary level of the injury. A person with an incomplete injury may

be able to move one limb more than another, may be able to feel parts of the body that cannot be moved, or may have more functioning on one side of the body than the other [39].

The level of injury dictates what parts of the body might be affected by paralysis and loss of function. However, it is very important to remember that in incomplete injuries there will be some variation in these prognoses. Cervical (neck) injuries usually result in quadriplegia. Injuries above the C-4 level may require a ventilator for the person to breathe. C-5 injuries often result in shoulder and biceps control, but no control at the wrist or hand. C-6 injuries generally yield wrist control, but no hand function. Individuals with C-7 and T-1 injuries can straighten their arms but still may have dexterity problems with the hand and fingers. Injuries at the thoracic level and below result in paraplegia, with the hands not affected. At T-1 to T-8 there is most often control of the hands, but poor trunk control as the result of lack of abdominal muscle control. Lower T-injuries (T-9 to T-12) allow good trunk control and good abdominal muscle control. Sitting balance is very good. Lumbar and sacral injuries yield decreasing control of the hip flexors and legs. Aside from a loss of sensation and movement, patients with a spinal cord injury may also experience bladder (see section below) and bowel complications [39].

1.2.3 The effects of Spinal Cord Injury on Urinary Bladder

As described in section 1.1.5, nerves near the end of the spinal cord (the sacral level of the spine) control the urinary system. The spinal cord injury does not affect the kidneys function or collection of the urine in the bladder. The changes that take place after an SCI, however, determine the function of the bladder and sphincter muscles. After a spinal cord injury, messages can no longer travel normally between the bladder or sphincter muscles and the brain. Therefore, individuals cannot feel when the bladder is full or they do not have the urge to urinate [40].

Initially after injury, no voiding occurs due to the presence of detrusor-sphincter dyssynergia (DSD) and patients must be catheterized [10]. This neurogenic disorder is a disruption of the usual coordinated relaxation of the external urinary sphincter with the contraction of the detrusor. Instead of relaxing, the external sphincter contracts further in response to a detrusor contraction. The detrusor then contracts against a closed sphincter so that no urine can exit. As a result, the majority of the SCI patients develop urologic complications. These complications include overactive bladders (due to detrusor hyperreflexia) and urinary retention (due to incomplete voiding), which can lead to recurrent urinary tract infection and vesicoureteral reflux with or without upper urinary tract deterioration [40-43]. It has been also reported in literature that muscular hypertrophy and fibrosis in bladder wall occur in these neurogenic bladders, which, in turn, result in lower bladder compliance in chronic SCI patients [2, 8] (Table 1).

Table 1: General effects of spinal cord injury on the urinary bladder function [2, 8, 40-43].

| |
|-------------------------------------------------------------------------|
| Initial (2-12 weeks) shock phase no voiding; urinary retention |
| Increase in bladder weight throughout remainder of life |
| Hypertrophy of bladder smooth muscle cells throughout remainder of life |
| Resulting clinical conditions, any or all, (12 weeks – end of life) |
| Detrusor hyperreflexia (DH): overactive bladder |
| Detrusor-sphincter dyssynergia (DSD) |
| Decreased bladder compliance |

Generally, there are 2 types of abnormal voiding through which the bladder regains partial functionality after a spinal cord injury.

1. Spastic or reflex bladder

In some patients, two to twelve weeks after trauma, a reflex bladder response returns that restores at least involuntary bladder emptying. This response may result from collateral sprouting of new neural pathways, loss of an inhibitory influence of the injury, or emergence of more primitive alternative pathways [10, 44]. Spastic or reflex bladder means that when bladder fills with urine, a reflex automatically triggers the bladder to empty. The problem with a spastic bladder is patient does not know when the bladder will empty. He/she is also at greater risk for sphincter dyssynergia. Spastic or Reflex bladder usually occurs when the injury is above the T12 level [45].

2. Flaccid or non-reflex bladder

This means one's reflexes may be sluggish or absent. Patient may not feel when the bladder is full. It then becomes over-distended or stretched. This can cause the urine to back up through the ureters to the kidneys. Stretching also affects the muscle tone of the bladder. Individuals with injuries below T12/L1 usually have a flaccid bladder [45].

However, return of the reflex response does not mean normal bladder control. Bladder dysfunction caused by spinal cord injury does not improve through time. In fact, it usually gets worse and requires continuing, vigilant medical supervision and patient compliance with the prescribed routine [39].

2.0 REVIEW OF PREVIOUS STUDIES

2.1 FUNCTIONAL AND MECHANICAL PROPERTIES

Since the sole function of the bladder is to store urine under low pressure and expel it, the mechanical properties of the urinary bladder wall are clearly important in understanding its function (Figure 8). Generally, evaluation of the mechanical behavior of the urinary bladder at the tissue- and organ levels has provided useful information in assessment of the functional state of the organ [41-43, 46-49]. Since the bladder is a neuro-muscular organ, the mechanical evaluation and analyses must be carefully conducted by dissecting out respective neurogenic and myogenic influences (e.g. neural excitation, smooth muscle tone and spontaneous contraction) while exposing the specimen to controlled loading states that are realistic and quantifiable. Past studies have included quasi-static uniaxial [46, 50-52], *in situ* [46, 53-55], and uniaxial viscoelasticity studies [42, 46, 56, 57]. Although these techniques allow the bladder tissues to be isolated from neurogenic inputs and/or exposed to controlled mechanical loads, there are certain limitations. For example, uniaxial testing subjects bladder strips to loading in one direction only and leaves one edge stress-free, which is never the case *in vivo*. Whole organ testing is more physiological, but the complex stress and strain boundary conditions on the bladder wall, due, for example, to the external loading by the surrounding organs or its irregular geometry, prevents

from investigation of isolated tissue response. Thus, to evaluate the mechanical properties of a biological tissue, physiological testing protocols that subject the tissue to realistic in vivo forces and deformations should be used. It has been demonstrated that biaxial mechanical testing can be successfully used to investigate mechanical behavior of the urinary bladder wall [58]. Mechanical data was obtained from biaxial tests were based on a physiologic-like loading state, which allowed for a thorough experimental investigation of the physiological stress range. Furthermore, the appropriate constitutive models have been developed [59], and biaxial stress relaxation studies have been performed [60]. These studies have demonstrated that the urinary bladder wall mechanically behaves as an anisotropic, highly time-dependent biological tissue.

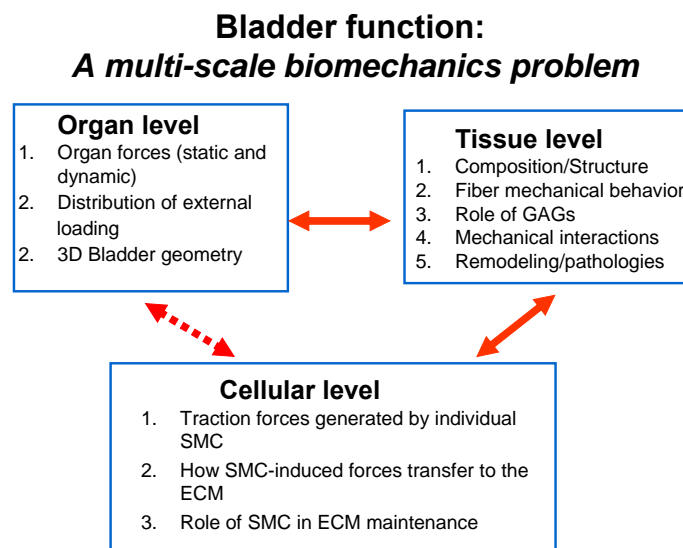


Figure 8: The overall current concept of bladder biomechanical function

2.1.1 Current Clinical Functional Evaluation: Cystometry and Urodynamics

Urodynamics studies are routinely performed in clinics to evaluate the health of the patients' bladder. The cystometrogram is an organ-level test in which the functional pressure-volume curve is recorded. A double-lumen catheter inserted through the urethra into the bladder is used

to fill the bladder and to measure intravesical pressure (Figure 9). This pressure-volume curve is compared against a standard and used to diagnose bladders that are noncompliant due to a variety of maladies. Variations on cystometry include natural cystometry or controlled slow cystometry (CSC), which use a filling rate closer to physiological urine output, one much slower than conventional cystometry [61, 62]. On the other end of the scale, rapid filling and step filling instead of constant rate filling have been used to obtain viscoelastic constants of the bladder wall [47, 63-66]. In addition, attempts have been made to quantify urinary bladder fiber strength [67] and the amount of work done by the bladder [68] using the pressure-volume relationship obtained from cystometry. To isolate the effects of nerve impulses on bladder function, sacral nerve roots have been identified and stimulated [69].

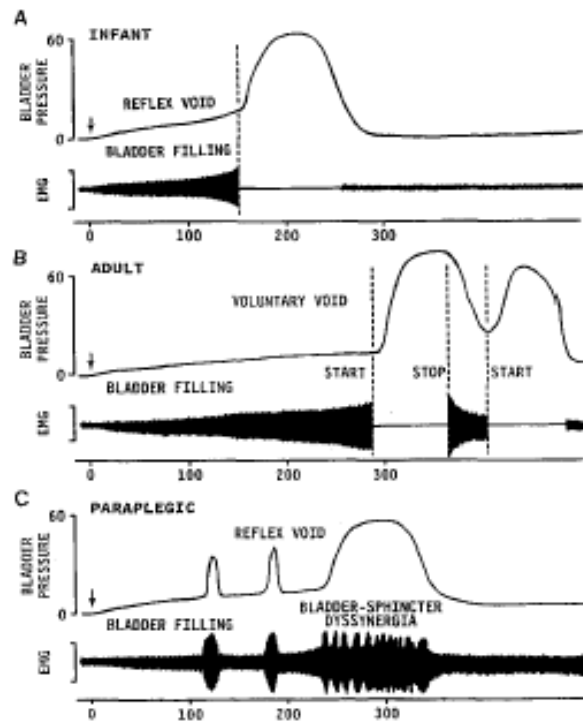


Figure 9: An example of combined cystometrograms and sphincter electromyograms (EMGs) comparing reflex voiding responses in an infant (A) and in a paraplegic patient (C) with a voluntary voiding response in an adult (B). The abscissa in all records represents bladder volume in milliliters, and the ordinate represents bladder pressure in cm H₂O and electrical activity of the EMG recording. On the left side of each tracing, the arrows indicate the start of a slow infusion of fluid into the bladder (bladder filling). Vertical dashed lines indicate the start of sphincter relaxation, which precedes by a few seconds the bladder contraction in A and B. In B, note that a voluntary cessation of voiding (stop) is associated with an initial increase in sphincter EMG followed by a reciprocal relaxation of the bladder. A resumption of voiding is again associated with sphincter relaxation and a delayed increase in bladder pressure. In the paraplegic patient (C), the reciprocal relationship between bladder and sphincter is abolished. During bladder filling, transient uninhibited bladder contractions occur in association with sphincter activity. Further filling leads to more prolonged and simultaneous contractions of the bladder and sphincter (bladder-sphincter dyssynergia). Loss of the reciprocal relationship between bladder and sphincter in paraplegic patients interferes with bladder emptying (Redrawn from [2]).

Another minimally invasive urologic test is the measure of bladder impedance correlated to bladder fullness is used in patients who have lost the ability to sense urinary fullness [70]. Echo planar imaging and Doppler sonography of the bladder emptying have been used to view the velocity of urine exiting the bladder [71, 72]. More complete studies include measurements of bladder wall thickness to normalize the pressure-volume data [69]; however, this cannot be used clinically as it involves removal of the bladder after cystometry.

Cystometrograms cannot directly determine bladder wall tissue properties, because these tissues have thickness and regional differences that cannot be reliably measured *in vivo*. Further, *in vivo* studies may be affected by neural influences and are always affected by intrinsic muscle activity, neither of which can be controlled. In general, *in vivo* evaluation is a function of the mechanical properties of the bladder wall, the non-uniform wall stress distribution, and external loading by the pelvic organs.

2.1.2 Intact Organ Testing *in vitro*

In *in vitro* whole-organ testing, the intact bladder is removed to isolate it from nervous stimulation and external loading. As in cystometry, the bladder is filled with a fluid and the resulting pressure-volume curve is examined [64, 73]. This test allows the researcher to control the environment of the bladder by introducing specific electrical impulses that affect muscle contraction [74]. Since the bladder is maintained as a three-dimensional fluid-containing sac as *in vivo*, the recorded parameters can be directly related to bladder function and its ability of the bladder to hold and void urine under specified conditions.

Although *in vitro* testing is relatively physiological and not confounded by the interaction of the other abdominal contents as are cystometry measurements, it still has the disadvantage of

variations and errors due to wall thickness and bladder shape, and the inability to apply a simple loading pattern or know with precision the loading pattern applied. Additionally, only a single control of either pressure or volume is available to the experimentalist. Rigorous mechanical analysis requires better control of the material and the ability to load the material in multiple dimensions.

2.1.3 Uniaxial Testing

A complete analysis of the mechanical properties of the bladder wall tissue can be conducted only when the tissue is isolated and all forces applied are known. This requires either knowledge of the exact shape and regional thickness of the intact bladder, both of which are invariably different from animal to animal, or isolation of sections of bladder wall in known and specific configurations. Many investigators have carried out controlled-force studies on isolated tissue using bladder strips. Alexander has used bladder strips to study the rat bladder in detail, applying load to a transverse strip of tissue [41, 46, 52]. Van Mastrigt and coworkers have studied human and guinea pig bladder in an isolated strip preparation [47, 65]. Much useful information has been gathered through strip uniaxial testing. Alexander found that when a high pressure is rapidly removed, there is a corresponding rapid decrease in length, indicating an elastic element in urinary bladder mechanics [46]. Macarak and others have found that after the detrusor layers were surgically removed, both in bladder strips and in intact bladders, the tissue samples became more compliant, indicating that the components of the muscle layers may serve to limit the total volume of the bladder, contributing to stiffness [20, 54] (Figure 10).

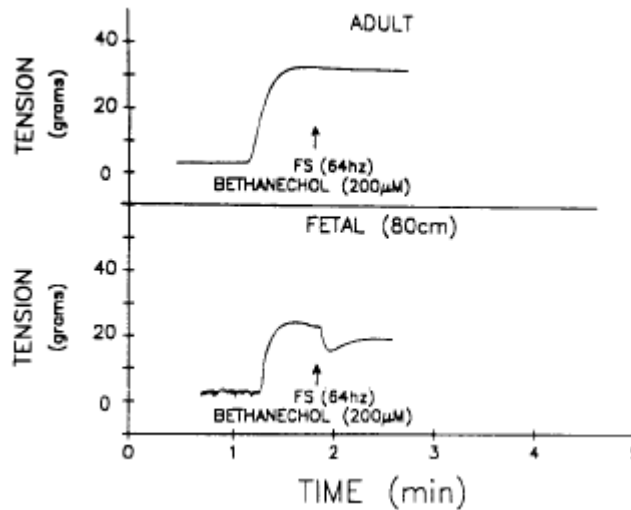


Figure 10: Representative response of isolated strips of fetal and adult calf bladder to field stimulation (64 Hz) following bethanechol prestimulation (200 μM) in a uniaxial testing. Arrows indicate initiation of field stimulation (Redrawn from [74]).

The numerical results of these tests are maximum tensions and other stress-strain relationship quantities. However, uniaxial testing cannot be used to fully describe the properties of the bladder, since the muscle bundles are not homogenous nor always of a predictable orientation [16]. In addition, to allow dissipation of the uneven stress concentrations at the gripped sample edges, deformation measurements are done in the center of the tissue and the specimen dimensions are typically 1:5 to 1:10 (width: length), resulting in a long, thin specimen. Cutting the tissue results in a reorganization of the fibers at the edges, yet due to the small width of the sample, measurements often need to be taken near the edge, resulting in large errors. Nevertheless, data obtained from uniaxial strip tests have been used to develop predictive models of bladder behavior. These models have been largely empirical, constructed to meet the criteria that the model fit the given data well. Most have been based on the classic spring (elastic) and dashpot (viscous) elements, incorporating three or four elastic and three or four viscous elements in each model [41, 43, 46, 47, 65]. The models may fit the data well, but the parameters that

result can only be compared to those of other tissues tested and fit in the same manner, to the same model. As in all phenomenological models, the parameters do not describe the intrinsic properties of the tissue and therefore cannot be used to learn anything about the tissue function or, more importantly, differences in tissue function due to abnormal states.

Baskin and coworkers devised a novel two-dimensional test in which a strip of material was sandwiched between two plates with a circular hole cut out of them. A pressure gradient was then applied across the cutout so the specimen bulged. The maximum pressure applied and the resulting deflection were then used to compute the stresses [32]. Although this test did remove the effects of the specimen geometry from the tissue testing, it still allowed only a single test. To obtain a complete description of the mechanical properties, multiple stress states with different stresses in both anatomical directions is required.

Uniaxial testing has revealed that the bladder is similar to other biological tissues. It undergoes a reduction in stress when held at constant deformation (stress relaxation). The behavior stabilizes after the first few cycles so that the first cycle is different from the subsequent stable cycles (preconditioning). There is measurable energy loss during each cycle (hysteresis). In addition, it has been shown that the rate of stretch does not affect the magnitude of tension developed [75].

2.1.4 Biaxial Mechanical Testing

Previous evaluations of the mechanical properties of bladder wall tissue have focused on testing strips of bladder tissue where a load is applied in one direction only, *i.e.* uniaxial testing [46, 50-52]. Uniaxial testing isolates the tissue and subjects it to controlled stress states, but it is non-physiologic since it leaves the edges completely stress-free, a state that never occurs *in vivo*.

Physiological loading of the bladder wall is both tensile and compressive, and includes components in all three dimensions. Tensile tissue loads are in the plane of the tissue while compressive loads oriented perpendicular to the bladder surface are induced by urine and surrounding pelvic structures. For thin, virtually incompressible membranes like the bladder, a planar biaxial state of stress is sufficient to fully describe the three-dimensional tissue mechanical properties [76, 77]. In biaxial testing, the thickness must be significantly smaller than the lateral dimensions. Biaxial mechanical testing therefore allows for a more realistic physiological loading state. Further, by varying the loads in each orthogonal axis the complete mechanical behavior of the bladder wall over the entire normal and pathological range of function can be determined.

Gloeckner *et al* reported the first studies of quasi-static planar biaxial mechanical testing applied to the bladder wall. In these experiments, three different states were utilized to evaluate the bladder wall tissue response: passive-, active-, and inactive-states [58, 78, 79]. The passive-state and active-state tests were performed in the presence of calcium with either smooth muscle tone only (passive) or with chemically induced contraction (active), while the inactive-state tests were conducted in the absence of calcium from the solution with no smooth muscle contractile activity. Thus far, it has been demonstrated that the inactive-state tissue compliance of 10-day SCI rat bladder wall under biaxial stress was significantly greater compared to normal bladders [58]. Furthermore, 10-day SCI rat bladder changed its material class following spinal cord injury and behaved as an isotropic material while normal rat bladder was mechanically anisotropic [58].

In addition to the changes in compliance and material class, Nagatomi *et al* investigated the viscoelastic behaviors of normal and spinal cord injured (SCI) rat bladder wall tissue using planar biaxial stress relaxation tests [60]. Bladders from normal and spinalized (3 weeks) rats

were subjected to biaxial stress (either 25 kPa or 100 kPa in each loading direction) rapidly (in 50 ms) and subsequently allowed to relax at the constant stretch levels in modified Krebs's solution (in the absence of calcium; with no smooth muscle tone) for 10,000 seconds. It was observed slower and therefore less stress relaxation in the SCI group compared to the normal group, which varied with the stress-level (Figures 11a and 11b). These experimental results were successfully fitted ($R^2 > 0.98$) to a reduced relaxation function [80]. Collagen and elastin, in general, are considered stiff and compliant extracellular elements, respectively, of soft tissues such as bladder wall. In terms of their viscoelastic responses, however, elastin relaxes very little, much less compared to smooth muscles or collagen [80]. In other words, elastin, which is easily distended under small forces, does not dissipate stored energy as readily as collagen and smooth muscle (Figure 11c). The SCI rat bladders exhibited similar amount of collagen but increased amounts of smooth muscle and of elastin compared to normal bladders. These changes in the composition and mechanical properties of bladder wall may be a compensatory mechanism triggered by non-physiological mechanical conditions of the bladder following spinal cord injury; bladder smooth muscles of SCI populations are subjected to increased work load due to overactivity and to chronic over distension due to outlet obstruction. In particular, it is possible that the increased amount of elastin in the SCI bladders may be responsible not only for the reduced stress relaxation, but also for the increased compliance of the bladder wall, which can allow large distension as well as reduce work load of smooth muscle [60].

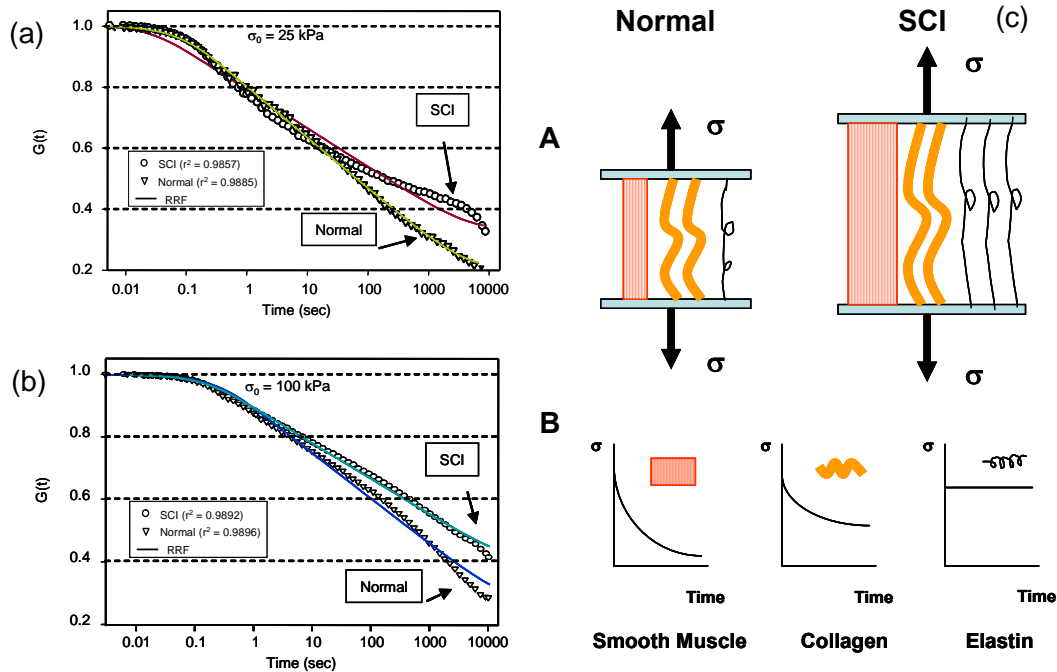


Figure 11: The reduced relaxation function $G(t)$ applied to stress relaxation data of normal and SCI bladders for a peak biaxial stress of (a) 25 kPa and (b) 100 kPa. The model fitted the data for both groups successfully ($R^2 > 0.98$). (c) Schematic representation of the bladder as composite structures under stress relaxation. Compared to the normal rat bladders, SCI rat bladders contained more smooth muscle and elastin, but similar amounts of collagen. As a result, SCI bladders exhibited increased distensibility and decreased rate of stress relaxation. This is due to different viscoelastic behaviors of smooth muscle, collagen, and elastin, which exhibits large, medium, and virtually no stress relaxation, respectively (Redrawn from [60]).

These results demonstrated the capability of planar biaxial testing to examine functional and mechanical changes in the urinary bladder, and suggested that SCI and the associated urologic functional changes induce profound tissue remodeling, which, in turn, provided the structural basis for the alterations in the time-dependent mechanical behavior of the urinary bladder wall.

2.2 STRUCTURE AND MORPHOLOGY OF THE BLADDER WALL IN SCI

2.2.1 Bladder enlargement and muscular hypertrophy

One of the most obvious results of acute SCI is increased bladder size. This can be seen as a rapid increase in wet weight of the urinary bladder to two to three times as much as the control in only 7 days [3]. The bladder enlargement is mainly due to muscular hypertrophy (Figure 12). The detrusor layer thickness increases from 100-120 μm in normal to 250-300 microns in SCI bladders [16].

Interestingly, upon microscopic analysis of SCI patient tissue, not all smooth muscle cells are found to be hypertrophied, as would be expected if this phenomenon were only an effect of pressure [3]. One explanation for this phenomenon is that the hypertrophy is caused by an alteration or lack of stimuli from peripheral autonomic nerves and that only smooth muscle cells with nerve receptors are affected, leaving the cells that receive their nerve signals from adjacent cells unaffected. Other investigators, however, have found that all muscle cells are directly innervated in the bladder [16].

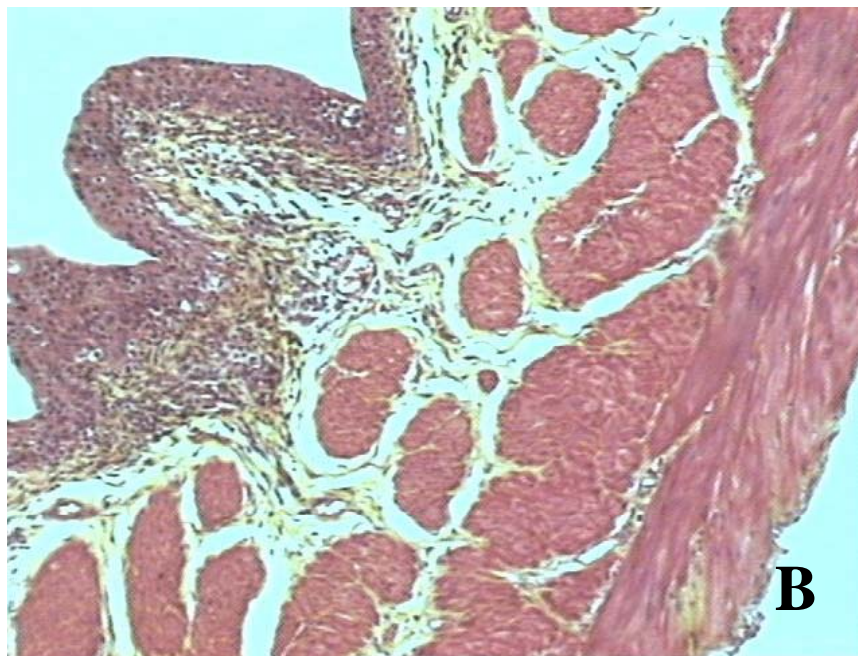
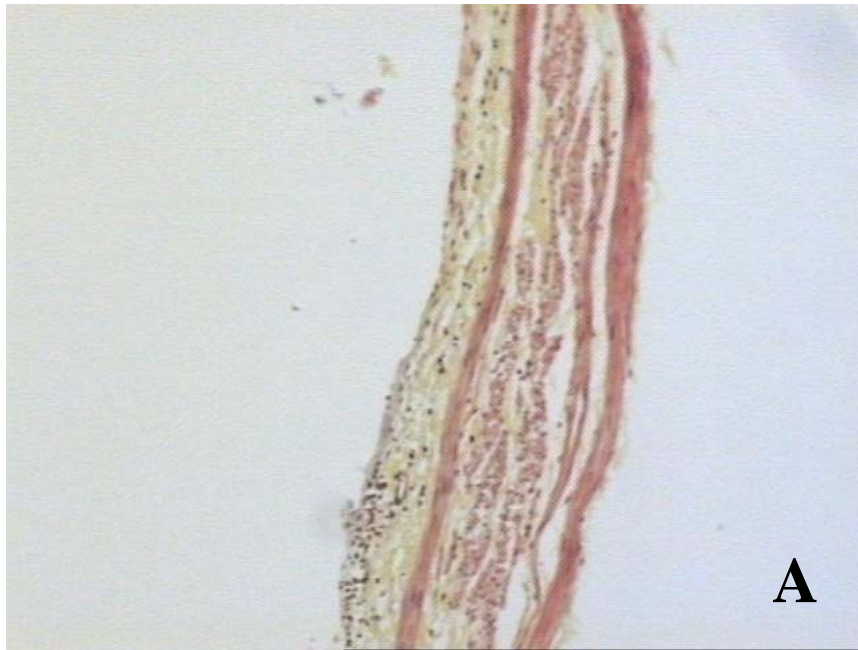


Figure 12: Photomicrographs of histological slides of the normal (A) and 10-day SCI (B) rat bladders, stained with Movat Pentachrome technique, mag. 10X. Both structural layers of bladder wall, lamina propria and detrusor, are significantly thicker in SCI sample when compare to the normal (Redrawn from [60]).

2.2.2 Area fraction and orientation of smooth muscle bundles in SCI bladders

Using a novel image analysis software, Nagatomi *et al* were first to quantify structural and compositional changes in the urinary bladder after spinal cord injury [81]. It was demonstrated that there were significant increases in smooth muscle and decreases in collagen area fractions in the 10-day SCI bladders compared to the normal group (Figure 13) [81]. Furthermore, the SCI bladders exhibited significantly fewer cell nuclei per muscle area compared to the normal bladders (Figure 14) [81].

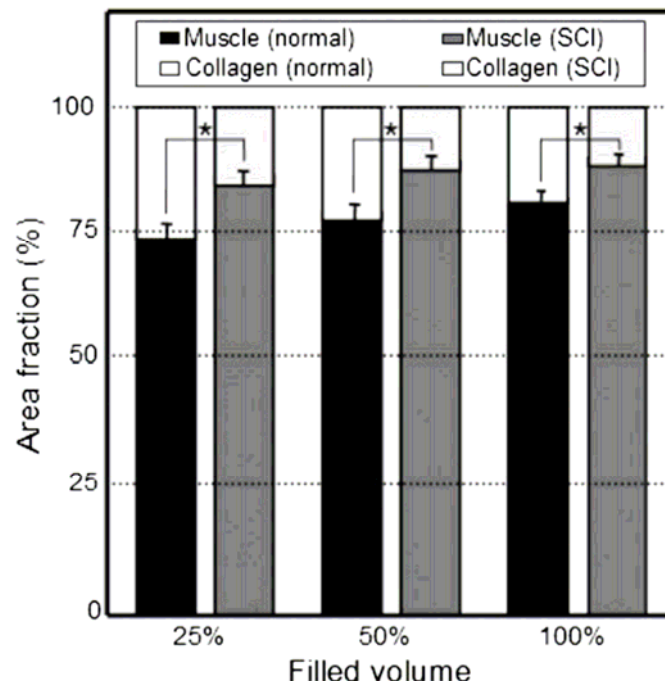


Figure 13: Area fractions of muscle and collagen in normal and 10-day SCI rat bladders at different volume levels. The SCI bladders exhibited significant (* $p < 0.05$) increases in smooth muscle and decreases in collagen area fractions compared to the normal bladders at all the volume levels examined. Data are mean \pm SD; $n = 5$; analyzed by Two-way ANOVA followed by the Student-Newman-Keuls post-hoc test (Redrawn from [81]).

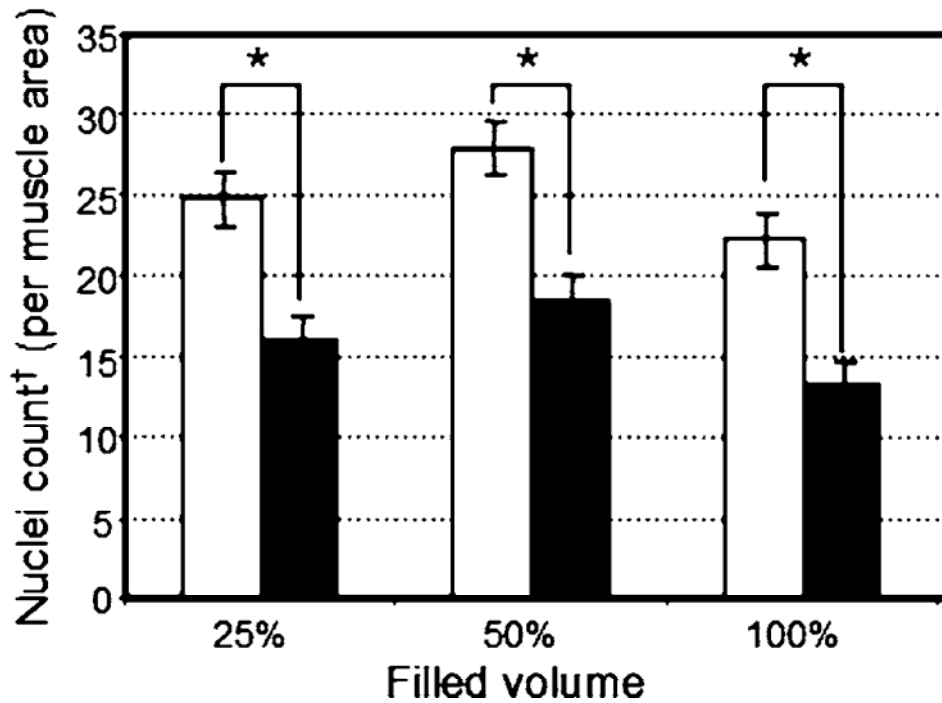


Figure 14: Nuclei counts of smooth muscle cells in normal and 10-day SCI rat bladders at different volume levels. The SCI bladders (black columns) exhibited significantly (* $p < 0.001$) fewer cell nuclei per muscle area compared to the normal bladders (white columns). Data are mean \pm SD; $n = 15$; analyzed by Two-way ANOVA followed by the Student-Newman-Keuls post-hoc test. † The values are normalized by the area fractions of muscle (Redrawn from [81]).

These results corroborated previous reports in the literature that the total collagen content of the bladder wall tissue (normalized by the wet tissue weight) decreased significantly following spinal cord injury, and suggested that the decreased collagen fraction in 10-day SCI rat bladders might contribute to, at least in part, the increased compliance of SCI rat bladders [58]. Furthermore, the fewer cell nuclei per normalized smooth muscle area in 10-day SCI rat bladder specimens compared to the normal specimens (Figure 14), indicated that the hypertrophy rather than hyperplasia is the predominant mechanism that led to the overall increase in the wall tissue thickness and mass [81].

In addition to the smooth muscle hypertrophy, 10-day SCI rat bladders exhibited a different pattern of muscle orientation distribution compared to the normal. Specifically, the orientation of smooth muscle bundles was bidirectional (*i.e.* in longitudinal and circumferential directions) in SCI bladders 10 days after injury, while the orientation of smooth muscle bundles in normal bladder was predominantly longitudinal (Figure 15) [81]. These results correlated well to the previous findings in biaxial mechanical testing of the bladder wall tissues (discussed in Section 2.1.4) [58]. Particularly, the change in overall muscle bundles orientation from predominantly longitudinal in the normal bladder to bidirectional in 10-day SCI bladder [81] corroborated the alteration in the material class between normal and 10-day SCI rat bladder wall tissues [58]. The smooth muscle bundles of the normal bladders exhibited predominant orientation in the longitudinal direction, which resulted in the orthotropic material behavior observed in the biaxial mechanical testing. Those of the 10-day SCI bladders, however, exhibited more biaxial orientation, which resulted in the isotropic behavior observed in the mechanical testing.

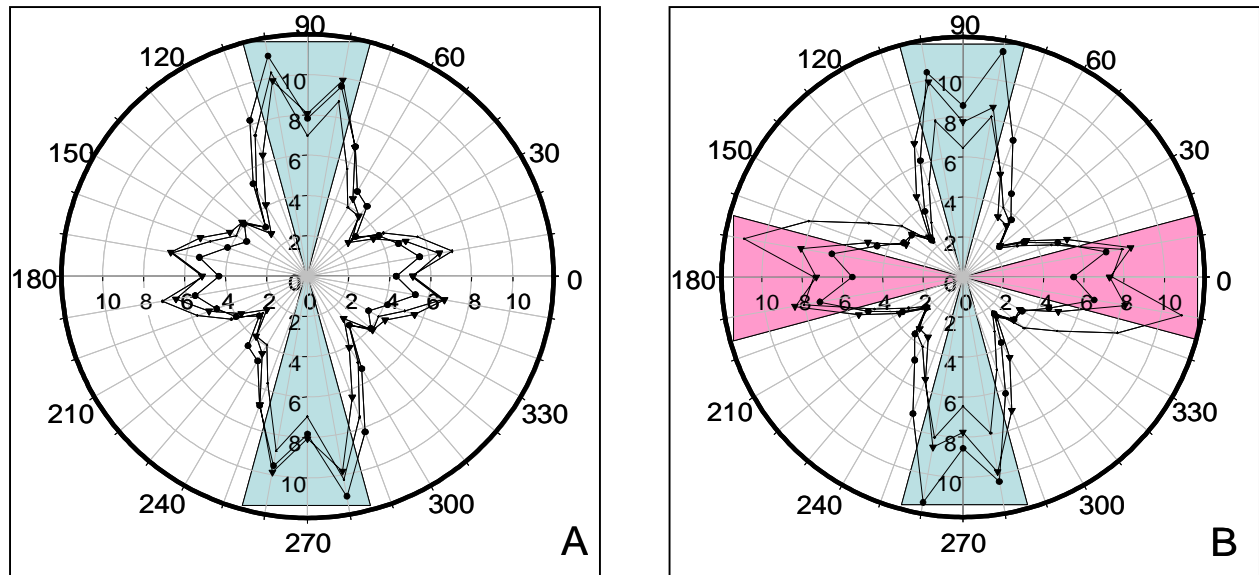


Figure 15: The orientation distribution of muscle bundles in normal and SCI rat bladders. In the normal bladders (A) the predominant muscle orientation was along the longitudinal axis, while the 10-day SCI bladders (B) had predominant muscle orientation along both longitudinal and circumferential axes at all volume levels examined (● 25%, ○ 50%, ▽ 100%). Colored triangles represent longitudinal (blue) and circumferential (red) biases (Redrawn from [81]).

2.2.3 Changes in collagen content

The relative amounts of type III and type I collagen have been found to change after spinal cord injury. One study found that while normal rat bladder collagen type III and type I contents are 25% and 75%, respectively, in the post-injury bladder, progressive fibrotic changes increased the percentage of type III to 33% [20, 23]. This change is also associated with alterations in mechanical compliance in bovine studies [12]. Throughout this change, however, the distribution of the connective tissue components (collagens I and III and elastin) in the lamina propria did not change in noncompliant bladders [24], suggesting that most of the alterations were within the detrusor layer.

It is interesting to note that in most tissues, fibrosis is characterized by overproduction of collagen type I, not type III as is seen in the urinary bladder [4]. This holds true even for tissues that have a high type III content in their normal state, such as the kidney and liver [82]. The fibrotic process within a noncompliant urinary bladder due to obstruction is therefore very unusual, at least within the detrusor [24]. Results of studies investigating changes in collagen content in humans differ. Some studies have found no significant difference in the total collagen content between normal and non-neurogenic obstructed bladders in persons from 3 months to 68 years of age [18]. However, Deveaud and colleagues found a significant increase in collagen type III in both neurogenic and non-neurogenic noncompliant bladders but no significant change in type I [4]. Within the areas of neurogenic bladders classified as relatively normal, there were increased collagen levels but not elastin levels, indicating that elastin might be localized to damaged regions but collagen deposition is more uniform throughout the bladder wall [17]. In comparisons of neuropathic and non-neuropathic disorders, both collagen and elastin levels increased, but the increases were higher in neuropathic bladders (Figure 16) [17].

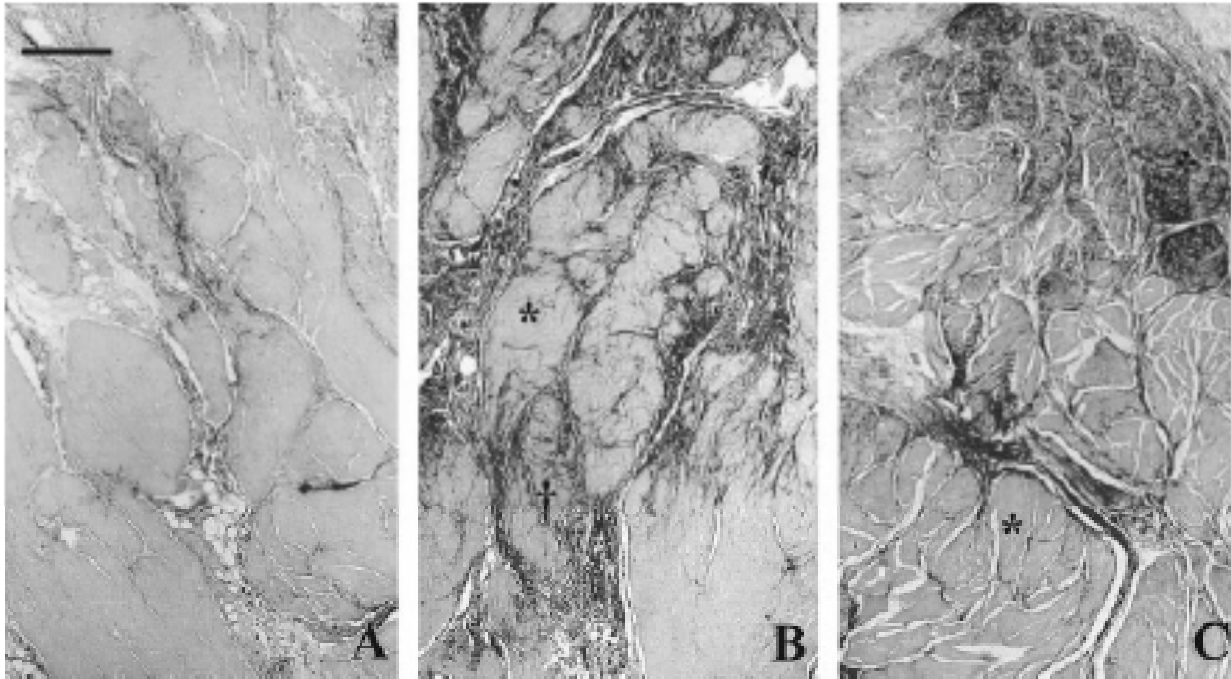


Figure 16: Photomicrographs of human detrusor bladder tissue from control (A), idiopathic (B), and neuropathic bladders (C). Normal areas are signified by *, and † indicates a severely affected area in B. The scale bar is 200 μm [17].

In general, the changes caused by similar pathological mechanism (*i.e.* bladder outlet obstruction) was first evident in the superficial detrusor layer next to the lamina propria, and then occurred deeper within the muscle layer, and finally resulted in the fibrotic effect over the full transmural thickness in noncompliant bladders [24]. This widespread fibrosis may result in an outward shift of the compliant layer from the lamina propria to the infiltrated smooth muscle layer in an overall noncompliant bladder [24].

2.2.4 Changes in elastin content

Using gene array analysis, Nagatomi *et al* demonstrated that there were significant early changes in the extracellular matrix protein genes of the rat detrusor following SCI [81, 83]. Briefly, the results of their molecular level study provided evidence that as early as 3 days following spinal cord injury the rat bladder tissue exhibited significant upregulation of genes encoding for tropoelastin, lysyl oxidase, TGF- β and IGF-1, which returned to the baseline level at 3 weeks.

In addition, biochemical studies of 3-week SCI rat bladders revealed major increase (approximately 8- to 10-fold) in the total amount of elastin content when normalized by the tissue weight [60]. While the trends were similar to literature reports on the changes in mechanically obstructed bladders, which increased elastin contents in rats and humans [84, 85], these findings were the first to demonstrate such changes in SCI rat bladders, and suggested that the resulting increase in the tissue compliance might be a compensatory mechanism to avoid excessive tissue injuries due to over distension of the bladder following SCI (Figure 17) [60].

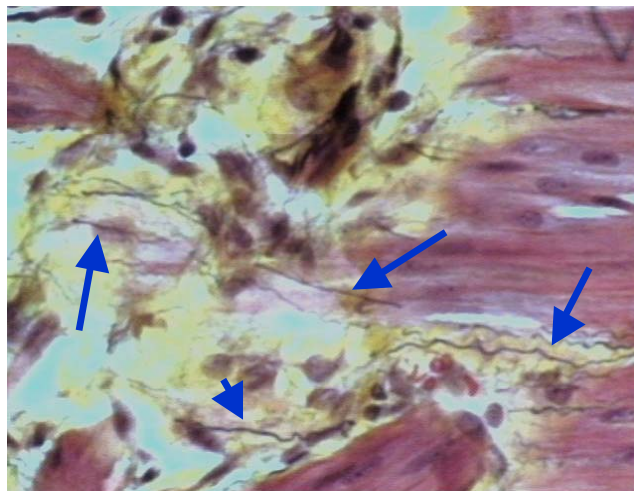


Figure 17: Digital images of a histology slide of 10-day SCI rat bladder, stained with Movat Pentachrome technique, mag. 40X. Increased amount of elastic fibers (stained in black; indicated by arrows) is notable (Redrawn from [60]).

2.3 SUMMARY OF CHANGES IN BLADDER TISSUE 10 DAYS AFTER SCI

In summary, previous biomechanical studies on the spinal cord injured bladders revealed significant changes in mechanical properties of rat bladder wall as early as 10 days after SCI, including increased tissue compliance, less stress relaxation, and shift in material class from anisotropic (in normal bladder) to isotropic (in 10-day SCI bladders) [58]. Furthermore, initial examination of histology sections of SCI rat bladders exhibited profound tissue alterations, which included smooth muscle hypertrophy and increased number of elastic fibers following spinal cord injury [60]. The image analyses of normal and 10-day SCI rat bladders demonstrated change in overall muscle bundles orientation from predominantly longitudinal in the normal bladder to bidirectional in 10-day SCI bladder [81], which corroborated the alteration in the material class between normal and 10-day SCI rat bladder wall tissues [58]. Finally, biochemical analyses provided additional evidence of significant changes in the extracellular matrix protein contents in SCI rat bladder [60]. These results demonstrated significant bladder wall tissue remodeling within 10 days following spinal cord injury and suggested that the mechanical behavior of the urinary bladder was strongly influenced by the tissue architecture and the amounts of extracellular matrix components.

2.4 HYPOTHESIS

It has been shown that changes in the mechanical environment of the bladder due to SCI can cause alteration in cellular compartment, such as smooth muscle hypertrophy, and in extracellular matrix, including ECM protein synthesis, as discussed in previous section. These changes in cell fate and matrix metabolism, in turn, could lead to alterations in bladder tissue composition and structure, which would, consequently, determine bladder functional properties (Figure 18). Based on the previous findings and current literature, it was hypothesized that bladder wall mechanical compliance is influenced by changes in ECM protein components, and bladder tissue material class is dictated by orientation of smooth muscle bundles.

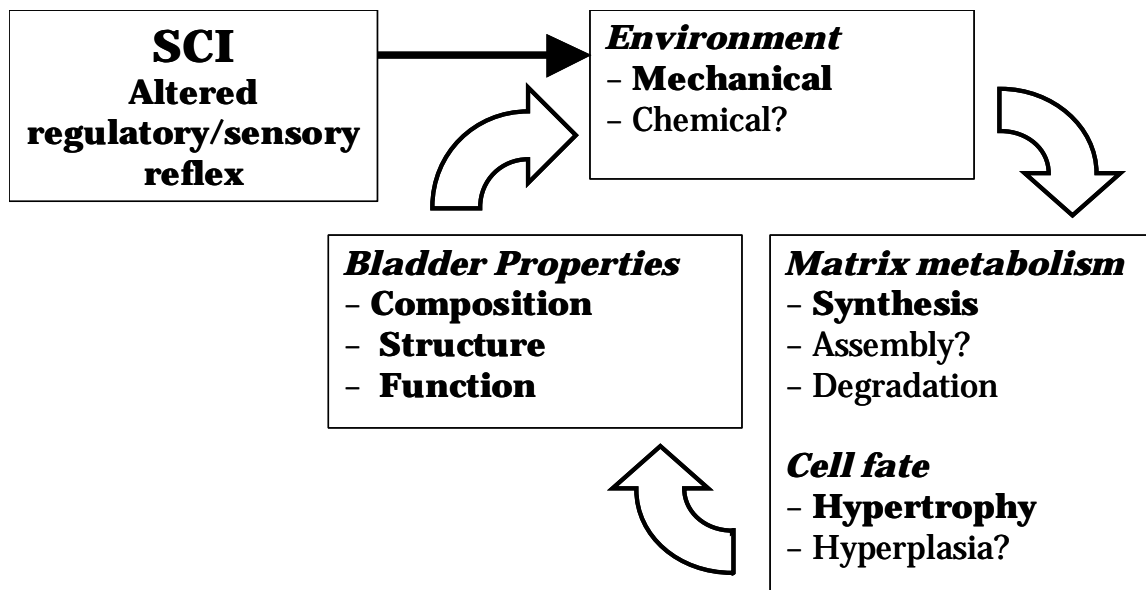


Figure 18: The altered mechanical environment of the urinary bladder following spinal cord injury, the key signal for the changes in the tissue functional properties.

2.5 OBJECTIVES

In order to test this hypothesis, the present study combined different experimental methods (including mechanical testing, biochemical assays and histomorphometry) to investigate changes in mechanical properties, as well as alterations in composition and morphology of the bladder wall tissue in an extended period of time following SCI.

2.5.1 Extension of timeframe to 10 weeks after injury

The reported studies in recent literature have primarily focused on the changes in bladder tissue shortly after the injury. These findings, however, were not quite consistent with clinical reports. For instance, increased compliance in 10-day SCI rat bladder contrasted typical, non-compliant bladder conditions found in chronic SCI patients [1]. Nevertheless, these short-term results only represented changes in early stages after injury, which were not necessarily comparable or consistent with chronic findings. In order to gain a deeper understanding of the changes in mechanical properties of bladder wall tissue, the investigation should be extended beyond the timeframe previously tested. The present study, therefore, was conducted at various time points up to 10 weeks after injury to evaluate time-course effects of spinal cord injury on bladder wall tissue.

2.5.2 Planar biaxial mechanical testing

As discussed in previous sections, biaxial mechanical testing has been successfully used to determine mechanical and functional properties of biological tissues, including urinary bladder. Biaxial testing allows for a nearly realistic physiological loading state, and by varying the loads

in each orthogonal axis, it provides the opportunity to determine the complete mechanical behavior of the bladder wall over the entire normal and pathological range of function.

2.5.3 Histomorphometry

Previously, Nagatomi *et al*, using a novel image analysis software, quantified structural parameters, such as smooth muscle bundles distribution and mass fraction of ECM proteins in the bladder wall tissue. This histomorphometric method demonstrated some unique features, and was proved useful to explain changes in material class from anisotropic in native bladders to isotropic in 10-day SCI bladders [81]. Therefore, this method was used in current study to follow up alterations in the distribution of smooth muscle bundles in 10-week SCI bladders, in order to correlate them to changes in the material class in those specimens.

2.5.4 Extracellular matrix proteins analyses

It has been extensively reported in literature, as discussed in sections 2.2.3 and 2.2.4, that ECM constituents play a major role in determining mechanical response of biological tissues. Collagen and elastin are, in particular, two molecular components in majority of soft tissues' extracellular matrix, which are responsible for the functional mechanical properties of the tissue. Specifically, changes in the protein contents in the 3-week SCI bladder tissue were reported to be consistent with the alteration of mechanical response in those specimens [60]. Therefore, ECM proteins analyses were also used in the current study to investigate correlation between changes in protein contents and mechanical response of SCI bladders up to 10 weeks after injury.

2.5.5 The overall goals

Extending the timeframe and combining various methods to study SCI rat bladders provides the opportunity not only to validate previous (*i.e.* so-called “short-term”) results, but also to investigate the structure-function relationship in the long-term SCI specimens to test the hypothesis, which was discussed above (see section 2.5.1). Specifically, the focus of interest was two major points. First, we were interested in finding out about bladder remodeling beyond the prior time points. In other word, based on previous findings, we expected to observe that bladder wall tissue continued to remodel and adjust with changes caused by spinal cord injury; meaning further alterations in the functional and structural properties of the bladder wall would be detected. Second, it has been suggested by existing literature that changes in matrix protein contents significantly affect mechanical response of the bladder tissue, such as its viscoelastic behavior [60]. Furthermore, changes in the structural properties can be responsible for alteration in mechanical characteristics of the bladder tissue. In particular, Nagatomi suggested that smooth muscle bundle orientation could be the determining factor to define the material class of the bladder wall tissue in 3-week SCI bladder [81]. The second main goal of this study, therefore, was to elucidate any potential correlation between structural/compositional properties, such as smooth muscle distribution and/or ECM proteins contents, and mechanical properties of the long-term SCI bladders, including material class and compliance.

3.0 METHODS

3.1 MECHANICAL CHARACTERIZATION

3.1.1 Specimen preparation

The protocol for creating spinal cord defects was identical to that used in prior studies in the urology and pharmacology laboratories [86, 87]. Female Sprague-Dawley rats (250-300g) were subjected to complete transection of spinal cord at the T9-T10 level. Under anesthesia, at the T9-T10 level the dura and spinal cord were cut with scissors and a sterile sponge was placed between the severed ends of the spinal cord. The bladders were emptied manually two to three times a day and general animal care was given according to our protocol approved by Institutional Animal Care and Use Committee (IACUC, University of Pittsburgh, Pittsburgh, PA). The whole urinary bladders were harvested at 3-week, 6-week, and 10-week (n=6 in each group) post-SCI and were immediately placed in modified Krebs's solution (containing 113 mM NaCl, 4.7 mM KCl, 1.2 mM MgSO₄·7H₂O, 25 mM NaHCO₃, 1.2 mM KH₂PO₄, 11.5 mM Glucose, and 1 mM EGTA, pH 7.4) and refrigerated at 4 °C for up to 48 hours following sacrificing of the animals.

Before mechanical testing, the bladders were cut open longitudinally along the urachus and were trimmed down to make square test specimens by removing the dome and trigone

sections of the organ (Figure 19A). Small carbon graphite particles were affixed on the luminal surface of the square bladder specimen for strain measurements and four sides of each specimen were tethered using suture and stainless steel hooks (Figure 19B). The test specimen was then mounted on a custom biaxial testing device (Figure 19C).

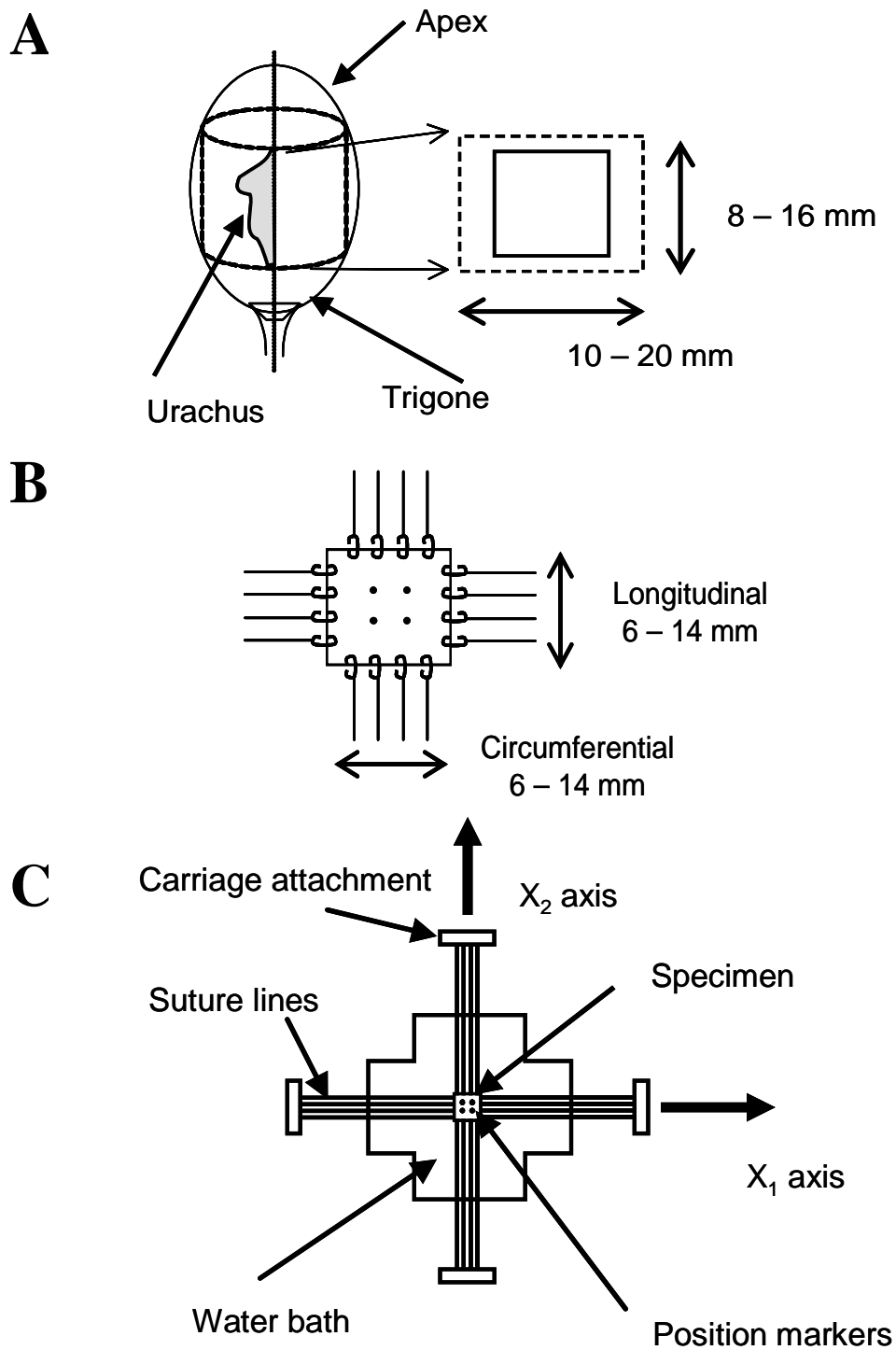


Figure 19: Rat bladders were cut open longitudinally along the urachus (panel A). Graphite markers were attached on the luminal surface (panel B). The test specimen was mounted on the biaxial testing device using stainless steel hooks and nylon suture lines (panel C).

3.1.2 Biaxial mechanical testing

Details of biaxial mechanical testing procedures and calculations have been described elsewhere [58, 76, 77]. Briefly, each side of the square test specimen was connected to the motor carriages *via* sutures to apply four-point loads (Figure 20). The load on each axis (circumferential and longitudinal) was constantly monitored using force transducers (with a signal conditioner) and the applied load was controlled by adjusting the stepper motors using our custom software and a data acquisition board installed on a PC. All specimens were tested at room temperature in the modified Krebs solution described.

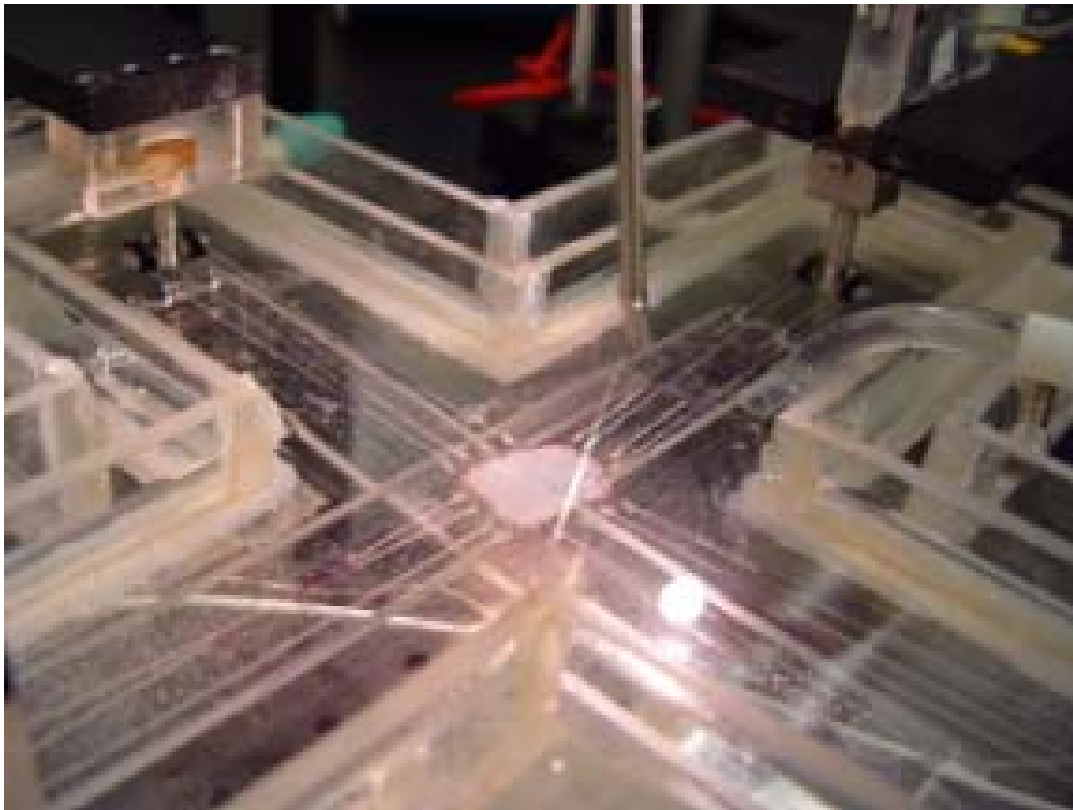


Figure 20: Image of sample attached to biaxial testing device through stainless steel hooks and nylon suture lines.

Stresses along the longitudinal and circumferential axes (T_L and T_C , respectively) were defined in the Lagrangian sense as force/unloaded cross-sectional area. Further, by varying the loads in each orthogonal axis the complete mechanical behavior of the bladder wall over the entire normal and pathologic physiologic functional range could be determined (Figure 21, Table 2).

Table 2: Protocol for all specimens. See Figure 21 for graphical representation.

| Protocol | Ratio ($T_C : T_L$) | Maximum Stresses (kPa) | |
|----------|-----------------------|------------------------|---------------------|
| | | Circumferential, T_C | Longitudinal, T_L |
| 2 | 0.5:1 | 50 | 100 |
| 3 | 0.75:1 | 75 | 100 |
| 4 | 1:1 | 100 | 100 |
| 5 | 1:0.75 | 100 | 75 |
| 6 | 1:0.5 | 100 | 50 |

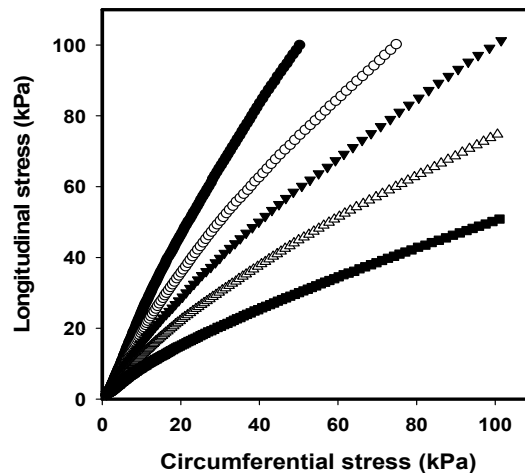


Figure 21: Stress-controlled biaxial mechanical protocols.

3.1.3 Data Analysis

Throughout testing, in-plane axial stretch was determined from the displacements of 4 markers affixed to the surface of the specimen (Figure 22). The following homogeneous biaxial deformation was considered:

$$x_1 = \lambda_1 X_1 + \kappa_1 X_2, \quad x_2 = \lambda_2 X_2 + \kappa_2 X_1, \quad x_3 = \lambda_3 X_3, \quad (1)$$

where \mathbf{X} and \mathbf{x} are the locations of material particles in the reference and deformed states, respectively, and λ_i and κ_i are the components of deformation tensor, \mathbf{F} (*i.e.* λ_i are the stretch ratios and κ_i measures of in-plane shear), which can be directly obtained at each time point during the test. Since soft tissues are composed primarily of water and have negligible permeability [80], they can be considered incompressible so that λ_3 is calculated from $\det \mathbf{F} = 1$.

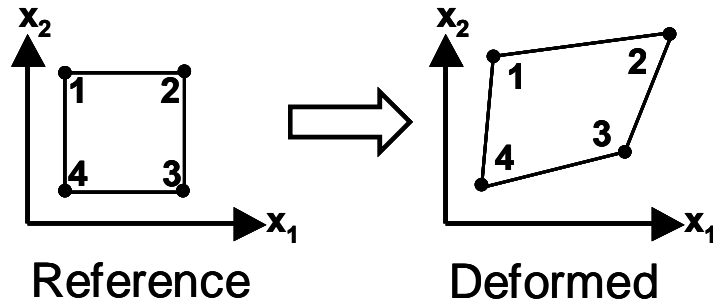


Figure 22: Mapping of the real-time positions of four tissue markers from the reference configuration to the deformed configuration, allowing for bi-linear interpolation of the displacement field (Redrawn from [76]).

The areal strain, representing the change in area between the reference and deformed states, was calculated. Areal strain incorporates stretch effects from the two axes and corresponds to net tissue mechanical compliance.

$$\text{Areal strain} = \lambda_1 \lambda_2 - 1 \quad (2)$$

Differences between groups were compared using an ANOVA analysis followed by a post hoc test of either Student-Newman-Keuls's test (where normality exists) or Dunn's procedure (when sample sizes were not equal). Data were presented as mean \pm SEM, and the difference was considered significant if $p < 0.05$.

3.1.4 Response Function

In this section, the mechanical data obtained in section 3.1.2 is used to fit in a mathematical model. The quasi-static data is analyzed using a response function technique and the results used to determine the best phenomenological model for 10-week SCI bladder wall tissue to highlight the differences in material classification between these specimens and previously examined (*i.e.* normal and 10-day SCI) bladders [17].

It was assumed that bladder wall behaved as hyperelastic material based on the concept of hyperelasticity [80]. Central to this theory is the existence of materials that conserve any mechanical work that is done on them as strain energy. In other words, a hyperelastic material is conservative, so the work done on it does not depend on the path; work is stored as strain energy in the material [88, 89]. Therefore, the in-plane 2nd Piola-Kirchhoff stresses \mathbf{S} could be derived from a scalar strain energy function W through:

$$\mathbf{S} = \frac{\partial W}{\partial \mathbf{E}} \quad (3)$$

where \mathbf{E} is Green-Lagrangian strain tensor. Since the stress-strain behavior of preconditioned specimens undergoing either loading or unloading was assumed pseudoelastic, in the sense that there is one stress state for each strain state [80], only loading data were utilized for the fit,

although both load and unloading data were recorded. Furthermore, shear strains and stresses were neglected as the data demonstrated very low values of shear.

In order to estimate the stress response to an arbitrary loading path within the experimental range, data obtained from all test protocols (i.e. with different loading ratios in two axes) were fit to interpolation functions. In all cases the biaxial protocols were fit simultaneously so that a wide region of strain states was included in the fit to avoid multiple colinearities [80].

Stress components in two main axes were computed using the following interpolation functions:

$$S_{11} = \frac{C_{10}}{2} (2c_{11}E_{11} + 2c_{13}E_{22} + 2c_{14}E_{11}E_{22} + c_{15}E_{22}^2 + 2c_{16}E_{11}E_{22}^2 + 4c_{17}E_{11}^3) \exp P_1 \quad (4)$$

$$S_{22} = \frac{C_{20}}{2} (2c_{22}E_{22} + 2c_{23}E_{11} + 2c_{25}E_{22}E_{11} + c_{24}E_{11}^2 + 2c_{26}E_{11}^2E_{22} + 4c_{28}E_{22}^3) \exp P_2 \quad (5)$$

where:

$$P_1 = c_{11}E_{11}^2 + c_{12}E_{22}^2 + 2c_{13}E_{11}E_{22} + c_{14}E_{11}^2E_{22} + c_{15}E_{22}^2E_{11} + c_{16}E_{11}^2E_{22}^2 + c_{17}E_{11}^4 + c_{18}E_{22}^4 \quad (6)$$

$$P_2 = c_{21}E_{11}^2 + c_{22}E_{22}^2 + 2c_{23}E_{11}E_{22} + c_{24}E_{11}^2E_{22} + c_{25}E_{22}^2E_{11} + c_{26}E_{11}^2E_{22}^2 + c_{27}E_{11}^4 + c_{28}E_{22}^4 \quad (7)$$

and c_{ij} are fitted parameters and E_{ij} are the components of Green strain tensor.

Each stress component was fit with a different parameter set with an excellent fit. Stress component contours over the experimental strain plane were generated to allow direct examination of material symmetries and to evaluate the material classification. The results of the response function analyses were used to determine which material class (e.g. isotropic, orthotropic, transverse orthotropic) was most applicable by examining the intricacies of the contour plots.

3.2 HYSTOMORPHOMETRY

Histological sections of the 10-week SCI rat bladders were imaged and analyzed according to the published methods [81].

3.2.1 Specimen preparation

Urinary bladders were harvested as whole from 10-week SCI ($n = 3$) rats under halothane anesthesia, which was immediately followed by euthanization of the animals with carbon dioxide. The ureters were ligated with silk sutures and each bladder was fixed by instillation of buffered formalin at 50% volume capacity and by submersing the formalin-filled bladder in another container of formalin overnight. A rectangular piece (5mm wide \times 8mm long) from the posterior part of each bladder was, following paraffin embedding, sectioned *en face* (approximately $5\mu\text{m}$ thick) throughout the thickness of the bladder wall (Figure 23) and stained using the Movat's Pentachrome technique. The time point and the region of the bladder from which these tissue sections were obtained were selected to be identical to those used in our previous mechanical studies in order to correlate the tissue morphology and mechanical behavior of bladder wall [81].

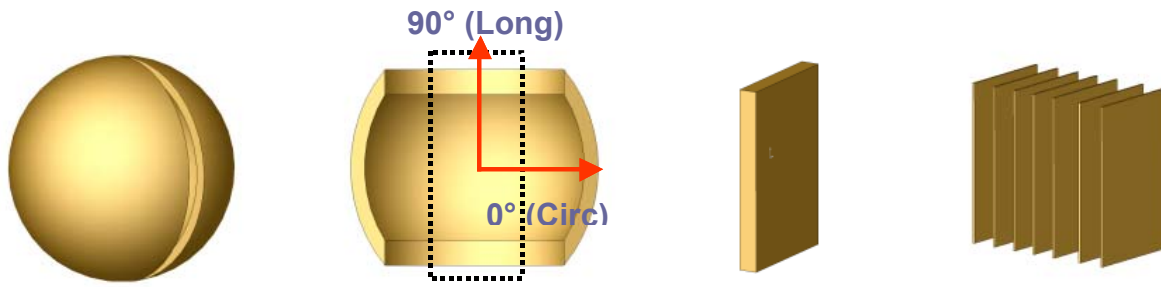


Figure 23: Schematic representation of the bladder histology specimen preparation. (a) The rat bladders were fixed in formalin under the filled condition at various volume % (25%, 50%, and 100%) overnight and cut open longitudinally along the urachus on the anterior (ventral) side; (b) a rectangular section was cut from the posterior (dorsal) side directly opposite of the initial cut; (c) a uniform size (5mm × 8mm) sections were embedded in paraffin; and (d) each piece was sectioned en face (approximately 5 μ m thick) throughout the thickness of the bladder wall and stained using the Movat’s Pentachrome technique (Redrawn from [81]).

3.2.2 Imaging of Rat Bladder Histological Sections

The details of this method have been described elsewhere [81]. Briefly, for each bladder specimen, 12 histological sections from the detrusor layer were examined using light microscopy (Nikon Eclipse, Nikon Corporation, Japan). On average, 6 fields (each covering an area of 1.14 mm × 0.91 mm) per section were imaged capturing the entire section (with average area of 8mm²) without any overlap between the image fields (Figure 24A). Digital images (640 × 512 pixels each) of these captured fields were obtained using a digital camera (SPOT RT, Diagnostic Instruments Inc., Sterling Heights, MI), and stored on a PC in PNG (Portable Network Graphics) format (Figure 24B).

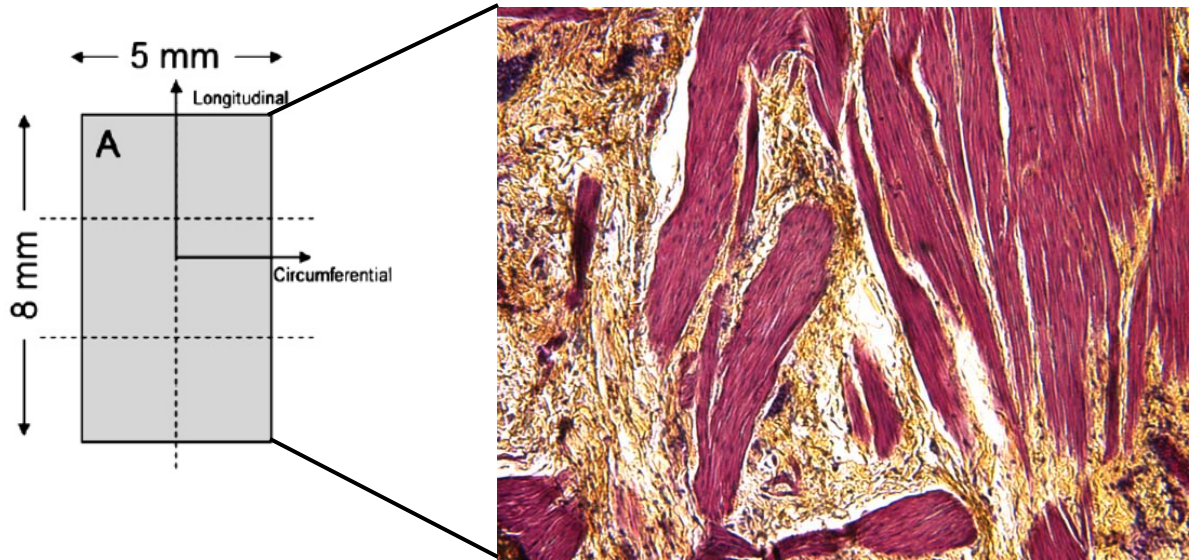


Figure 24: (A) Schematic showing the regions on the tissue section where the images were taken from (Redrawn from [81]); (B) Example image of a 10-week SCI bladder section, stained with Movat Pentachrome technique, mag. 10X.

3.2.3 Muscle Orientation

Histological sections of the 10-week SCI rat bladders were analyzed according to the published methods [81]. Briefly, the smooth muscle bundle orientation for each bladder was quantified by first grouping the muscle edge counts (obtained from 72 images per specimen) into 18 angular bins, such that each bin contained the number of edges that lay within an angle span of 10° (*i.e.* $-5^\circ-4^\circ$, $5^\circ-14^\circ$, $15^\circ-24^\circ$, . . . , $165^\circ-174^\circ$). The muscle edge counts in each angular bin were then normalized by the total number of muscle edges for each bladder, and the data were reported as edge count percentages, plotted in the polar coordinate system. In order to provide a visual clarity, taking advantage of the rotational symmetry of muscle orientation about horizontal axis (*e.g.* 30° is equal to 210°), the 180° -rotated image of the plot was added to the original graph to construct a 360° polar plot (Figure 29).

The mean smooth muscle orientations of 10-week SCI bladders ($n = 3$) were analyzed by performing the one-way analysis of variance using a commercial statistics software package (SigmaStat; SPSS Inc., Chicago, IL). This was followed by the Student-Newman-Keuls post-hoc test to perform pairwise comparisons of all the means. The p -values of less than 0.05 were considered statistically significant. Finally, the results were compared with that of the normal and 10-day SCI bladders reported by Nagatomi *et al* [81].

3.2.4 Tissue Composition

Using a novel image analysis method [81], the area fractions for tissue components were quantified in 10-week SCI bladder samples. The details of this method have previously published [81]. Briefly, the numbers of color-segmented pixels in each digital image, representing different components (*i.e.* red for muscle and yellow for collagen), were counted for all samples. The individual pixel counts for each component were normalized by the total pixel counts of both components (sum of red and yellow pixels, representing the entire tissue section) for each specimen and the data were reported as percent tissue fractions.

The mean tissue component area fractions of 10-week SCI bladders ($n = 3$) were analyzed by performing the one-way analysis of variance using a commercial statistics software package (SigmaStat; SPSS Inc., Chicago, IL). This was followed by the Student-Newman-Keuls post-hoc test to perform pairwise comparisons of all the means. The p -values of less than 0.05 were considered statistically significant. These results were also compared with that of the normal and 10-day SCI bladders reported by Nagatomi *et al* [81].

3.3 QUANTIFICATION OF EXTRACELLULAR MATRIX PROTEINS

3.3.1 Specimen preparation

Following biaxial mechanical testing the SCI bladder specimens were cut into 12 strips (1X10 mm each). These strips were weighed, and six of them were digested in 0.5N acetic acid supplemented with 1 mg/mL pepsin (Sigma, St. Louis, MO) at 4 °C overnight. Acid-soluble collagen in the supernatant solution was quantified using a commercially available assay kit (Accurate Chemical, Westbury, NY) and following the manufacturer's instructions. In order to digest elastin contents, the remainder six strips were treated with 0.25M oxalic acid at 95 °C for 180 minutes (60 minutes × 3). Elastin concentrations in these supernatants were also quantified using a commercially available assay kit (Accurate chemical) and following the manufacturer's instructions.

3.3.2 Data analysis

The data were expressed in terms of mass (in mg or μg) per volume of tissue specimen (in cm^3) analyzed by performing the two-way analysis of variance, when compared to that of normal and 3-week SCI bladders from a published study [60]. This was followed by the Student-Newman-Keuls post-hoc test to perform pairwise comparisons of all the means. The p -values of less than 0.05 were considered statistically significant.

4.0 RESULTS

4.1 MECHANICAL TESTING

4.1.1 Stress-stretch response

Response of a representative 10-week SCI bladder to various stress-controlled biaxial mechanical protocols is shown in Figure 25. These stress-stretch curves demonstrate that the longitudinal axis shows stretch reversal but the circumferential direction does not.

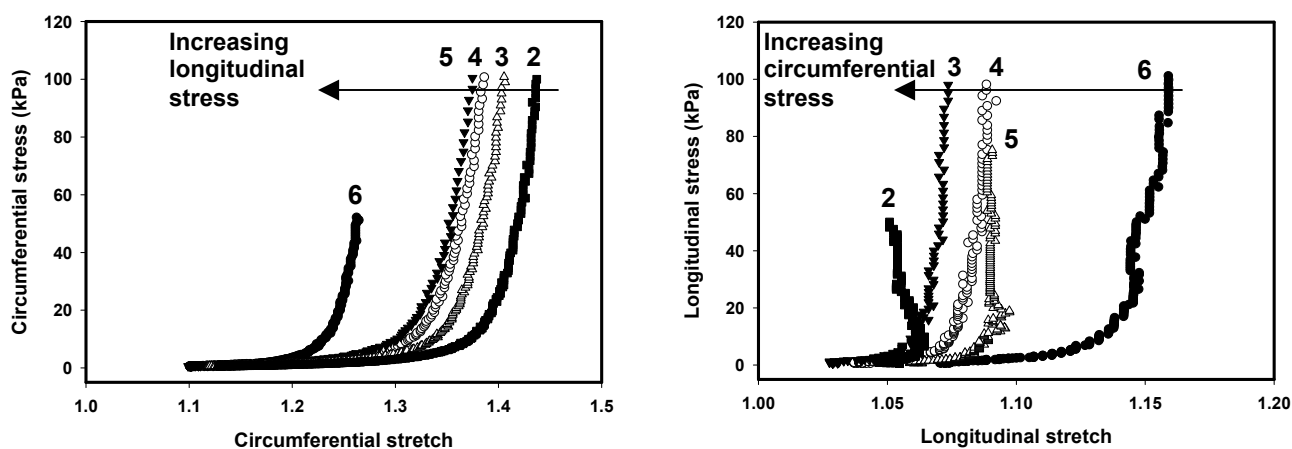


Figure 25: Representative stress-strain response to protocols listed in Table 3-2 for one normal specimen.

4.1.2 Changes in the areal strain

Biaxial testing of SCI bladder specimens in 3, 6, and 10 weeks following injury revealed that the bladder wall tissue compliance was significantly greater ($p < 0.001$) in 3-week and 6-week

samples compared to that of normal bladders (Figure 26). However, the compliance of 10-week SCI specimens was significantly lower ($p<0.001$) than 3-week and 6-week SCI samples, and was similar ($p=0.101$) to the tissue compliance of normal bladders.

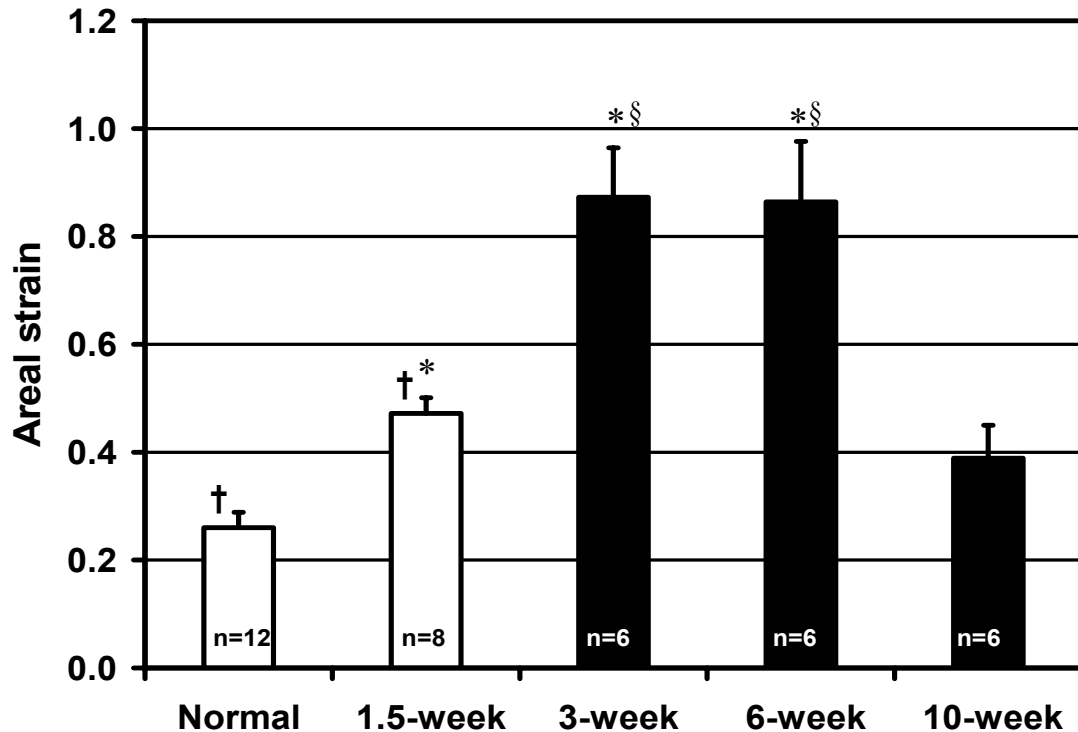


Figure 26: Changes in the mechanical compliance of the bladder wall up to 10 weeks after SCI. Areal strain, as an index of tissue compliance, was calculated (data are mean \pm SEM) in 3-week, 6-week and 10-week SCI specimens (* $p<0.05$, $n=6-12$, analyzed by ANOVA followed by Dunn's post-hoc test; † redrawn from [58], § redrawn from [17]).

4.1.3 Changes in the maximum axial stretches

Our results also demonstrated a significant difference between maximum axial stretch in circumferential and longitudinal directions in SCI samples. In particular, maximum axial stretch in circumferential direction was significantly ($p<0.05$) greater than that in longitudinal direction (Figure 27) in 3-, 6- and 10-week SCI bladders.

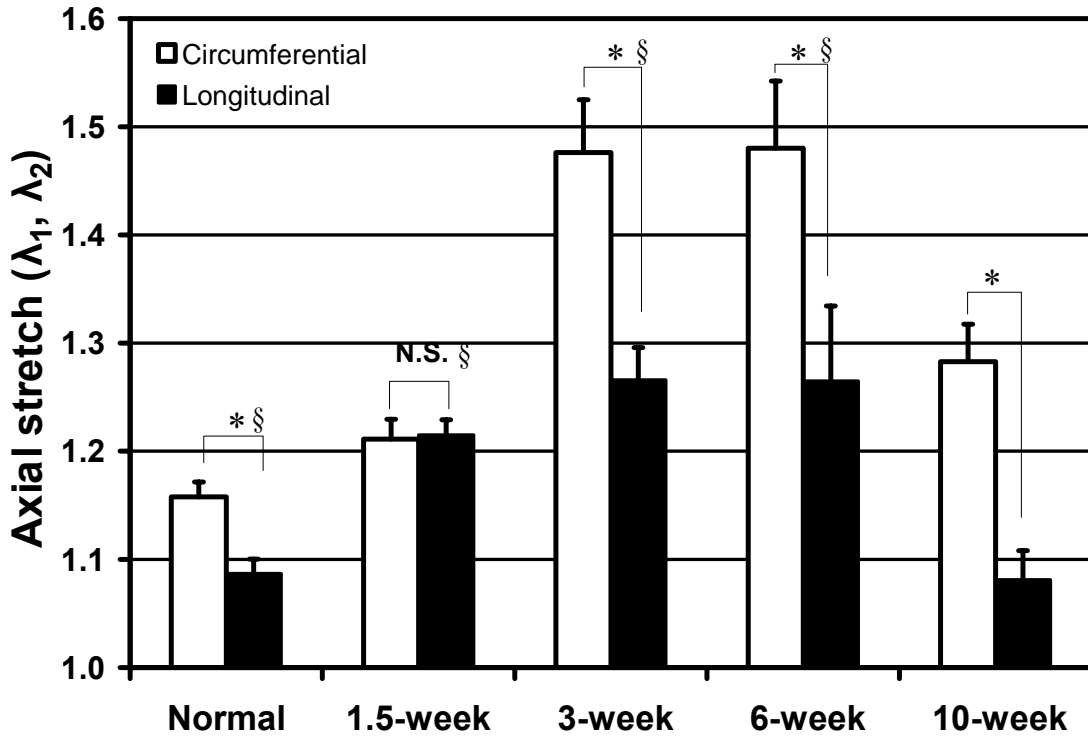


Figure 27: Biaxial mechanical response in the bladder specimens. Maximum axial stretches were determined in circumferential and longitudinal directions in normal and 1.5-, 3-, 6-, and 10-week SCI rat bladders (data are mean \pm SEM; * $p < 0.05$; $n = 6-12$; analyzed by ANOVA followed by a post hoc test; § redrawn from [17]).

4.1.4 Response function analysis

Response functions were viewed as two-dimensional stress component contour plots, which were generated over the experimental strain plane to allow direct examination of material symmetries to evaluate the material classification (Figure 28). The existence and direction of material axes were most apparent in the contour gradients plots of 10-week SCI, where there was marked lack of symmetry across the $E_{11} = E_{22}$ line, with the material axes strongly aligned to the x_1 (*i.e.* circumferential) stretch axes (Figures 28). Further, the distance between the contours was narrowed near the E_{11} axis compared to the E_{22} axis, indicating a strong dependence of W on E_{11} .

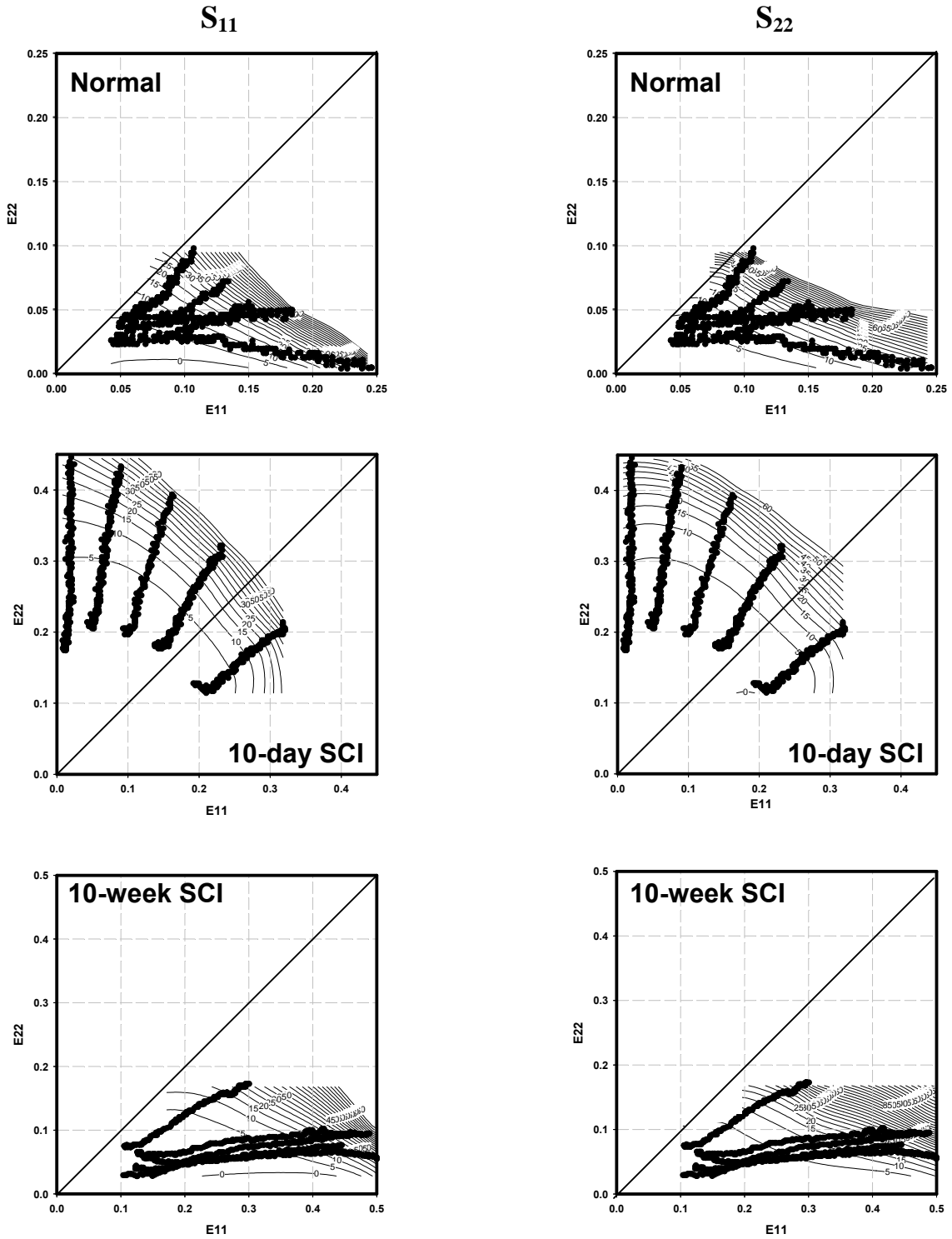


Figure 28: Stress contours for normal, 10-day SCI (redrawn from [17]), and 10-week SCI rat bladder wall, along with the actual strain values. Left column is designated to S_{11} and right column is for S_{22} . Solid diagonal lines are the $E_{11}=E_{22}$ identity, which is shown for visual reference.

4.2 HISTOMORPHOMETRY STUDY

4.2.1 Smooth Muscle Orientation

In the 10-week SCI rat bladders, muscle edge count percentages (representing the orientation of smooth muscle bundles) were extremely higher along the longitudinal axis of bladder. Specifically, the normalized muscle edge counts in 75° – 84° , 85° – 94° , 95° – 104° and 105° – 114° angle spans (with the mean ranging from $11.45 \pm 2.48\%$ to $17.88 \pm 3.34\%$) were significantly greater ($p < 0.05$) compared to those in all the other directions whose average values were less than 5% (Figure 29).

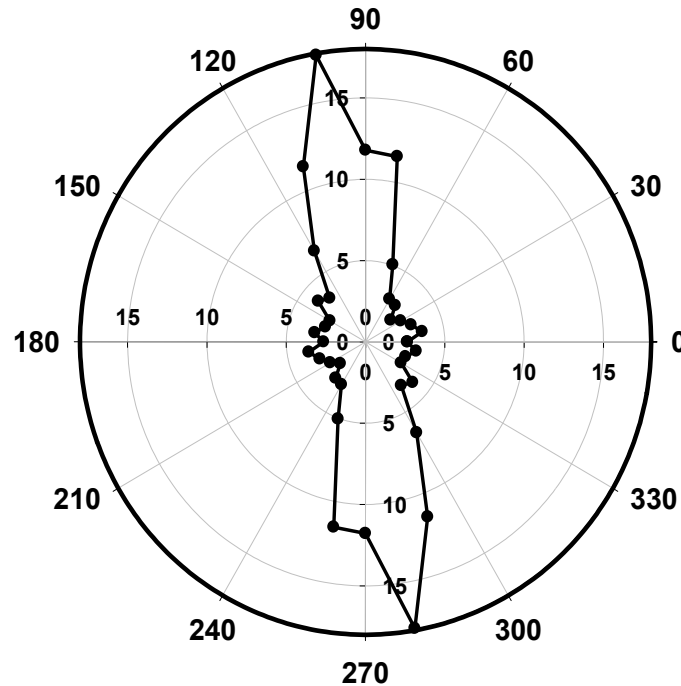


Figure 29: The orientation distribution of muscle bundles in 10-week SCI rat bladders, fixed at 50% volume capacity, $n = 3$.

4.2.2 Tissue Composition

Semi-automated image analyses of histological sections of rat bladder tissues revealed that the collagen area fractions in the 10-week SCI bladders were significantly ($p < 0.05$) higher compared to the 10-day SCI group, but were similar to the normal bladders (Figure 30).

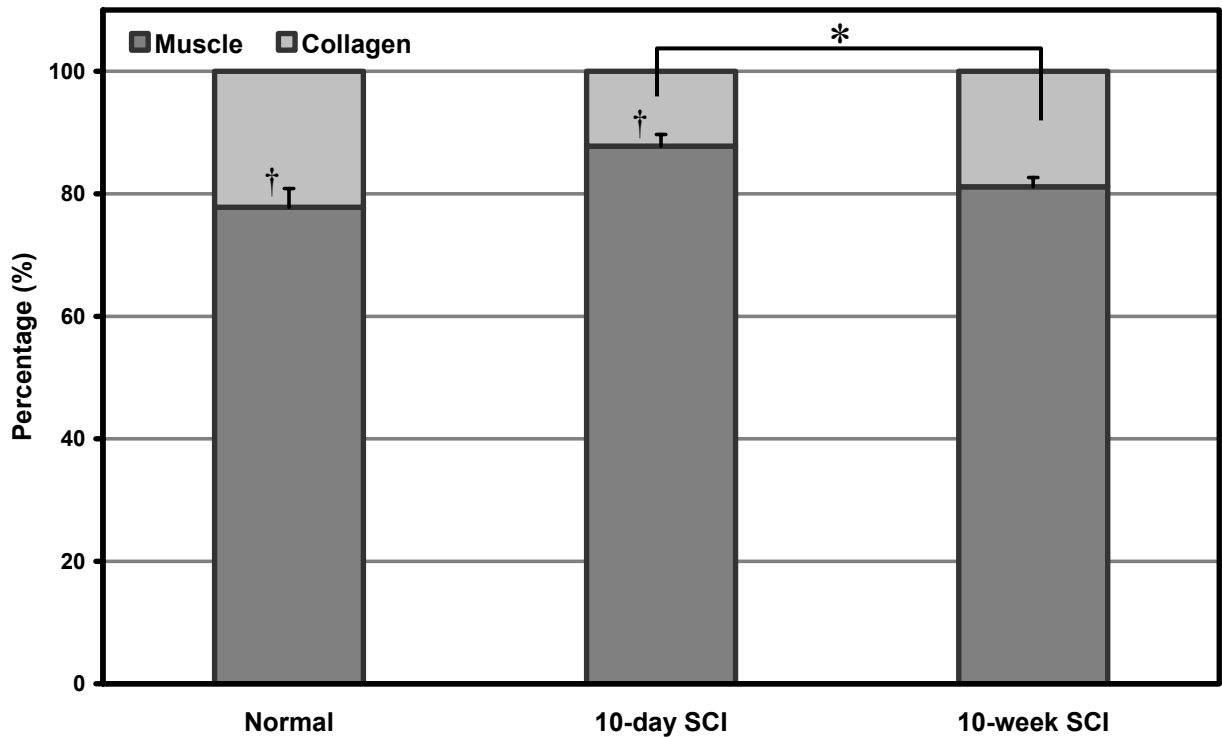


Figure 30: Area fractions of muscle and collagen in normal, 10-day and 10-week SCI rat bladders, fixed at 50% volume capacity. The 10-week SCI bladders exhibited significant ($* p < 0.05$) increases in collagen area fractions compared to the 10-day SCI group, but similar to the normal bladders. Data are mean \pm SD; $n = 3-5$; analyzed by One-way ANOVA followed by the Student-Newman-Keuls post-hoc test. † Redrawn from [81].

4.3 ANALYSIS OF MATRIX PROTEIN CONTENTS

The weights of SCI bladder specimens at all timepoints were significantly higher than those of normal bladders. Elastin contents of all SCI groups were also significantly higher than normal group. Collagen content was only statistically different in 10-week SCI bladder specimens (Table 3).

Collagen concentration (*i.e.* collagen mass normalized by volume of bladder specimen) of the 1.5-, 3-, and 6-week SCI rat bladders, expressed in terms of milligram per volume of tissue specimen, were statistically similar to each other, and were not significantly different when compared to the normal bladders collagen concentration (Table 4). The collagen concentration of 10-week SCI specimens, however, was significantly ($p<0.05$) greater than normal, 1.5-week, 3-week and 6-week SCI samples. Elastin concentration of the 1.5-, 3-, 6-, and 10-week SCI bladders, expressed in terms of microgram per volume of tissue specimen, were similar to each other, but significantly ($p<0.05$) higher than those of normal bladders (Table 4).

Table 3: Specimen weights, and collagen and elastin contents in the normal and SCI rat bladders (data are mean \pm SEM; * $p<0.05$; n=6-12; analyzed by one-way ANOVA followed by the Student-Newman-Keuls post-hoc test). † from [60].

| Group | Specimen weight (wet tissue, g) | Collagen content (mg) | Elastin content (μ g) |
|-------------------------|------------------------------------|--------------------------|-------------------------------|
| Normal [†] | 0.099 \pm 0.010 | 1.555 \pm 0.473 | 0.029 \pm 0.017 |
| 1.5-week SCI | 0.127 \pm 0.006 * | 1.316 \pm 0.220 | 0.105 \pm 0.031 * |
| 3-week SCI [†] | 0.162 \pm 0.019 * | 1.477 \pm 0.416 | 0.152 \pm 0.078 * |
| 6-week SCI | 0.130 \pm 0.016 * | 1.088 \pm 0.140 | 0.138 \pm 0.024 * |
| 10-week SCI | 0.211 \pm 0.017 * | 2.540 \pm 0.314 * | 0.218 \pm 0.026 * |

Table 4: Collagen and elastin concentrations, and elastin/collagen ratios in the normal and SCI rat bladders (data are mean \pm SEM; * $p < 0.05$; $n = 6-12$; analyzed by one-way ANOVA followed by the Student-Newman-Keuls post-hoc test). † from [60].

| Group | Collagen concent. (mg/cm³) | Elastin concent. (μg/cm³) | Elastin/collagen ratio (x100) |
|---------------------|--------------------------------------------------|----------------------------------------------------------------|------------------------------------------|
| Normal † | 25.913 \pm 2.982 | 0.481 \pm 0.092 | 1.86 |
| 1.5-week SCI | 21.927 \pm 1.636 | 1.742 \pm 0.229 * | 7.94 |
| 3-week SCI † | 24.612 \pm 2.623 | 2.541 \pm 0.530 * | 10.33 |
| 6-week SCI | 18.147 \pm 1.045 | 2.305 \pm 0.204 * | 12.70 |
| 10-week SCI | 42.341 \pm 2.621 * | 3.634 \pm 0.219 * | 8.58 |

4.4 SUMMARY OF FINDINGS IN 10-WEEK SCI BLADDER

In summary, biomechanical studies on the 10-week spinal cord injured bladders revealed significant changes in mechanical properties of rat bladder wall, including decreased tissue compliance (when compared to 3-, and 6-week SCI bladders), and shift in material class from isotropic (in 10-day SCI bladder) [58] to anisotropic. Furthermore, examination of histology sections of 10-week SCI rat bladders exhibited profound tissue alterations, which included smooth muscle hypertrophy, increased number of elastic fibers, and increased collagen content of the bladder wall tissue. The image analyses of 10-week SCI rat bladders demonstrated change in overall muscle bundles orientation from bidirectional in 10-day SCI bladder [81] to predominantly longitudinal, in a more pronounced pattern even when compared to the normal bladder, which was in agreement with the alteration in the material class between 10-day and 10-week SCI rat bladder wall tissues [58]. Finally, the biochemical analysis provided additional evidence of significant changes in the extracellular matrix proteins in 10-week SCI rat bladder, including significant increase in collagen concentration of bladder wall tissue.

5.0 DISCUSSION

5.1 BIOMECHANICAL ANALYSES

5.1.1 Changes in biomechanical properties of bladder wall

Previously, it was demonstrated that bladder wall compliance in 10-day SCI rats were significantly greater when compared to the normal bladders [58]. The results of present biomechanical study provided additional evidence that the compliance of the bladder wall tissue continued to increase up to 6 weeks following injury. The compliance, however, drastically decreased by 10 weeks after SCI and became similar to that of normal bladders (Figure 26). These findings suggest that bladder wall compliance may decrease even further for a period longer than 10-week post-injury, and bladder wall eventually becomes less compliant when compared to the normal bladders.

Furthermore, it was previously reported that the 10-day SCI rat's bladder tissue behaved as a quasi-isotropic material (*i.e.* exhibiting isotropic mechanical response under equi-biaxial loading) while normal rat bladder was mechanically anisotropic [58]. The results of present study, however, demonstrated that the maximum axial stretches in two anatomical directions were significantly ($p < 0.05$) different in 3-, 6- and 10-week SCI bladders when tested under

equibiaxial loading (Figure 27), indicating that bladder tissue behaved as an anisotropic material in those samples.

The alterations in the compliance of bladder wall tissue over a 10-week period of time post-SCI, and changes in material class from anisotropic (in normal rats) to isotropic (in 1.5-week SCI rats) to anisotropic (in 3-, 6-, and 10-week SCI rats) indicate that the mechanical properties of bladder tissue continuously change after spinal cord injury. These changes are in agreement with alterations in composition and structure of the 10-week SCI bladders, and support the existence of a close correlation between changes in structure /composition and mechanical properties of the bladder tissue.

5.1.2 Bladder wall model prediction

Although extensive modeling is not an objective of this study, it is desirable to evaluate biaxial mechanical properties independent of any specific constitutive model form. This is particularly the case when using stress-based biaxial mechanical protocols, which, although more convenient for quantifying the biaxial response within the physiological range, cannot be readily used to determine optimal constitutive model forms. In the present study, strain-energy interpolation functions were utilized in combination with stress-based biaxial testing data to determine changes in the material class and changes in degree and direction of mechanical anisotropy in the rat bladder wall 10 weeks after spinal cord injury [17].

The results of the response function analyses can be used to determine which material class (e. g. isotropic, orthotropic, transverse orthotropic) is most applicable by examining the intricacies of the contour plots. Symmetry across the $E_{11}=E_{22}$ line in a contour plot indicates isotropy, which may be modeled most efficiently with an isotropic function. Asymmetric plots,

requiring an orthotropic function, were examined to determine the larger strain axis, indicated by the majority of the strain region lying to one side of the line of symmetry and larger contour gradients. The most appropriate model choice for each group can ultimately be determined by examining the contour plots of each specimen and determining the dominant response.

The 10-week SCI samples demonstrated a complete asymmetry with more dependence of W on E_{11} when compared to the normal and 10-day SCI bladders. Conversely, the 10-day SCI samples with slight symmetry near the equi-strain line, exhibited a weak dependence on E_{22} . It was determined that the 10-week SCI group belongs to an anisotropic material classification, while 10-day SCI bladders wall were isotropic. The response functions proved useful for visualizing the stress response over a region of strain and were used for comparisons between the groups regardless of the particular strain values.

5.1.3 Tissue structural information and its relation to mechanical behavior

It is a very difficult task to directly evaluate the mechanical properties of biological tissues *in vivo*, therefore, defining any correlation between the tissue structure and its mechanical behavior becomes an alternative approach. The mechanical studies have demonstrated that the bladder wall exhibits complex biomechanical behaviors that are profoundly altered following SCI. In particular, Nagatomi *et al* have observed that the biomechanical properties (*e.g.* material classification) could be a direct result of rapid and profound bladder wall tissue remodeling, including changes in the bladder wall tissue architecture, such as smooth muscle cell orientation [81]. The results of the present study provided more evidence that changes in the orientation of smooth muscle bundles significantly contribute to the alteration in material class of bladder tissue (Figure 31). Specifically, when 10-week SCI bladder tissues were exposed to varying

ratios of non-equibiaxial loads, bladders exhibited strong influence of mechanical cross-coupling and behaved like anisotropic materials. This was consistent with the histomorphometric findings, which demonstrated dominant orientation of smooth muscle bundles along the longitudinal axis. Reviewing the previous results also reveals that dominant distribution of muscle bundles in longitudinal direction in normal bladders was mirrored by mechanical anisotropy in those specimens, and bimodal orientation observed in 10-day SCI bladders resulted in an isotropic behavior of bladder wall tissue (Figure 31).

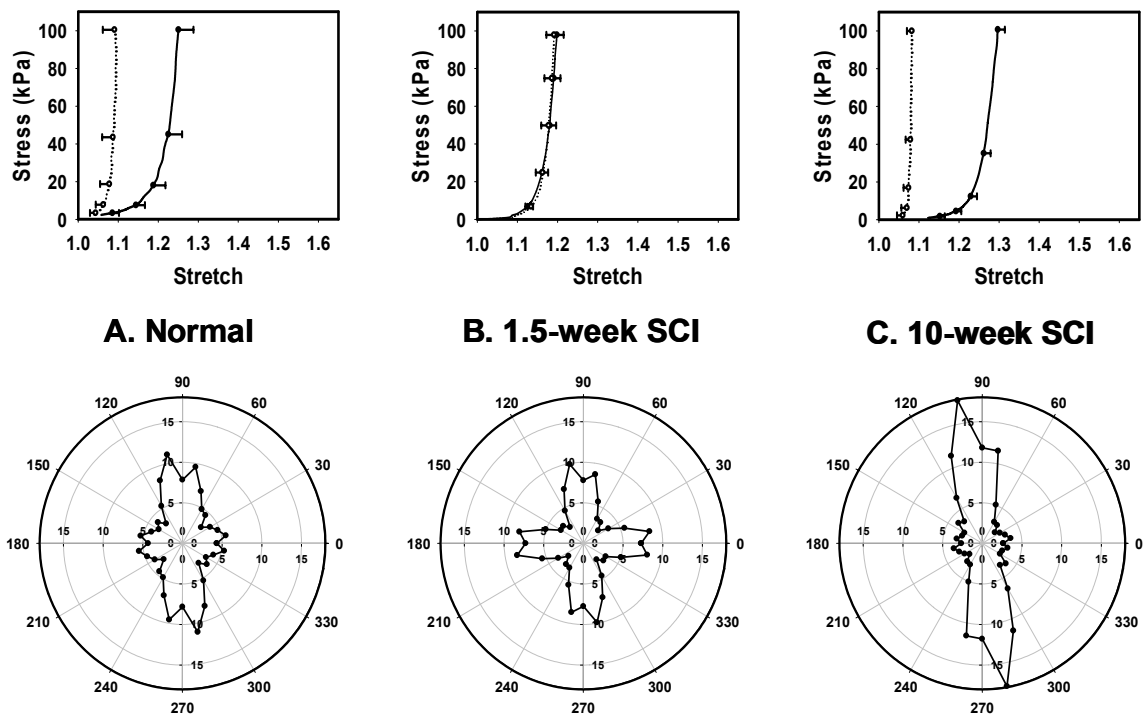


Figure 31: Comparison between results of mechanical testing and histomorphometry study. Upper panel: The longitudinal (\circ) and circumferential (\bullet) stress-stretch curves representing equibiaxial data (mean \pm SEM) in normal and SCI rat bladders indicated an isotropic response in 1.5-week SCI samples [17], but an anisotropic behavior in normal and 10-week SCI bladders. Lower panel: The orientation distribution of muscle bundles in normal (A), 1.5-week SCI (B) (redrawn from [81]), and 10-week SCI (C) bladders corroborated the mechanical anisotropy data.

5.2 MATRIX PROTEINS ANALYSIS

It has been postulated that the mechanical properties of the bladder wall are largely determined by the extracellular matrix components [15, 18, 85, 90]. In particular, collagen and elastin are two major connective tissue proteins providing tissues, including urinary bladder, with tensile strength and elasticity, respectively. Alterations in content or intrinsic properties of either of these proteins may lead to changes in bladder functional properties [15, 91].

The results of present study provided evidence that the SCI groups at all time points examined had higher elastin concentrations compared to the normal bladders (Table 3, Figure 32). This finding suggested that bladder tissue's early response to changes in mechanical environment (*e.g.* over-distension) occurred as early as 10 days after injury, and contributed to an increased compliance in 10-day SCI samples compared to the normal bladders. The collagen concentration of 10-week SCI bladders (when normalized by the tissue volume) was higher than normal and 1.5-, 3- and 6-week SCI rat bladders (Table 3), indicating a late response, which happened between 6 and 10 weeks post-injury.

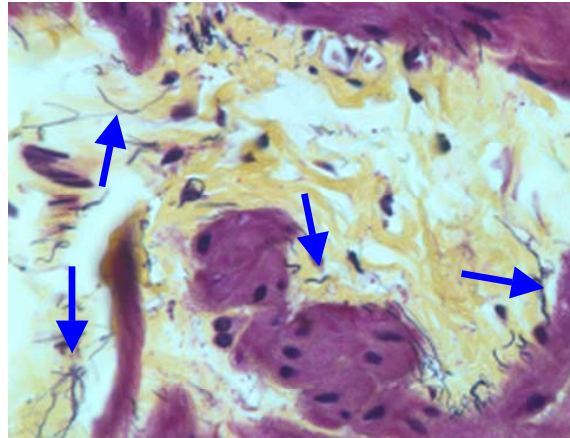


Figure 32: Digital image of histology slide 10-week SCI rat bladder, stained with Movat Pentachrome technique, mag. 40X. Increased amount of elastic fibers (stained in black; indicated by arrows) is notable.

Furthermore, the ratio of elastin/collagen concentration (normalized by tissue volume), as an index of relative changes in extracellular matrix, was calculated at each time point following injury (Table 3, Figure 33). This ratio has been suggested as an important factor in determining the compliance of the obstructed bladder [85]. The present results suggest a linear correlation (Figure 34), between elastin/collagen ratio and the compliance of the SCI bladders. Further biochemical analysis of the rat bladder wall, especially quantification of cross-linking for ECM proteins and/or collagen typing, will be, however, required to validate the link between alterations of the bladder compliance and changes in its composition following spinal cord injury.

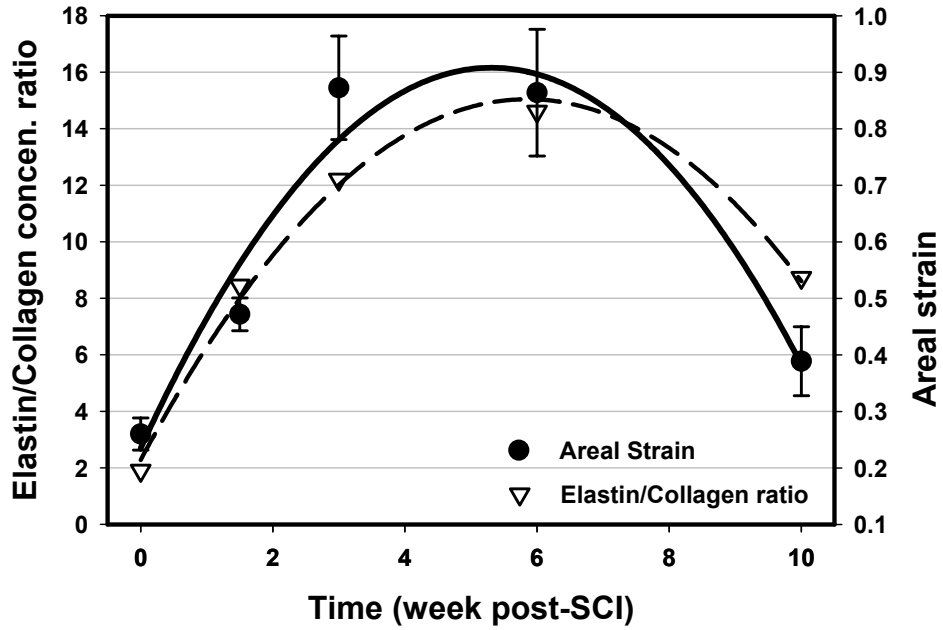


Figure 33: The changes in areal strain and elastin/collagen concentration ratio in rat bladder tissue over a period of 10 week after injury (those of normal bladder shown at zero time point). The similarity of two plots as a function of time suggests a potential correlation between them.

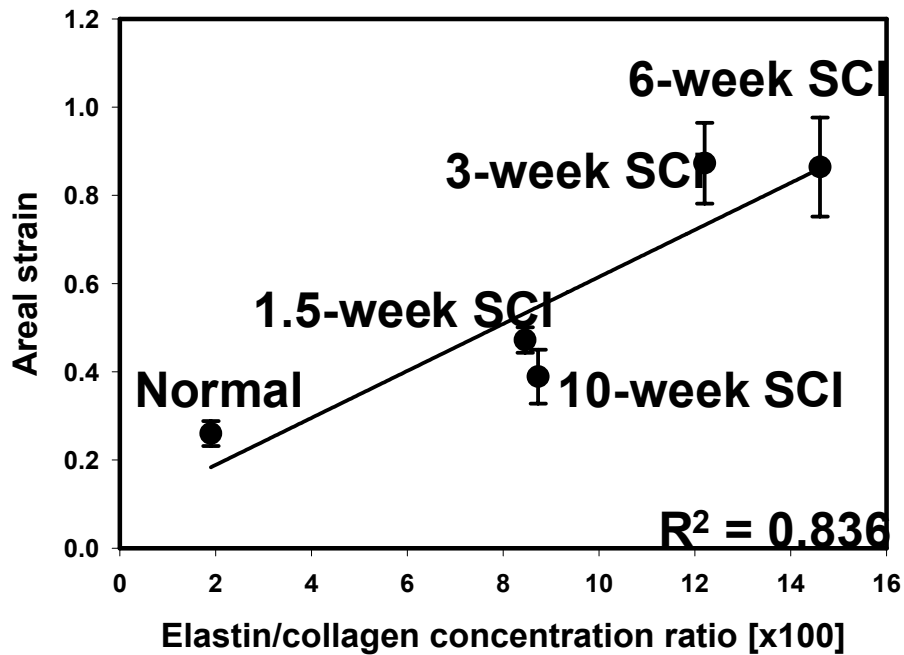


Figure 34: Areal strain at various time-points after injury plotted as a function of corresponding elastin/collagen ratio, exhibiting a linear correlation between them.

6.0 SUMMARY AND CONCLUSIONS

In this work, various experimental protocols and analysis techniques were combined to provide a thorough assessment of the changes in the urinary bladder wall 10 weeks after spinal cord injury.

6.1 CHANGES IN THE MECHANICAL PROPERTIES

Previously, Gloeckner *et al* demonstrated that bladder wall compliance in 10-day SCI rats were significantly greater when compared to the normal bladders [58]. The results of present study provided additional evidence that the compliance of the bladder wall tissue continued to increase up to 6 weeks following injury. The compliance, however, drastically decreased by 10 weeks after SCI and became similar to that of normal bladders. Based on these findings it can be speculated that bladder wall compliance may decrease even further for a period longer than 10-week post-injury, and bladder wall eventually becomes less compliant when compared to the normal bladders.

Furthermore, previous published study demonstrated that the 10-day SCI rat's bladder tissue behaved as a quasi-isotropic material (*i.e.* exhibiting isotropic mechanical response under equi-biaxial loading) while normal rat bladder was mechanically anisotropic [58]. The results of present study, however, exhibited that bladder tissue behaved as an anisotropic material in 3-, 6-, and 10-week SCI samples. The alterations in the compliance of bladder wall tissue over a 10-

week period of time post-SCI, and changes in material class from anisotropic (in normal rats) to isotropic (in 1.5-week SCI rats) to anisotropic (in 3-, 6-, and 10-week SCI rats) indicates that the bladder tissue continuously remodels after spinal cord injury. In addition, biomechanical analyses provided us with basic information that could be applied to develop constitutive models for SCI as a function of time, which can be utilized in computer simulations to predict mechanical response of the bladder in different time points after spinal cord injury.

6.2 CHANGES IN THE BLADDER WALL COMPOSITION AND STRUCTURE

While the overall pattern of compositional changes demonstrating tissue hypertrophy and increased elastin concentrations were similar to what have been reported in literature for similar pathologic conditions [84, 85], the present results are first to exhibit changes in spinal cord injured rat bladders, including increased collagen net contents by 10-week after injury, and correlation between tissue compliance and elastin/collagen ratio.

In the rat model of spinal cord injury, following the loss of voluntary voiding control due to the spinal transection, the rats normally gain the reflex voiding ability within the first 2–3 weeks. During this initial recovery period, however, the rats are unable to void urine without the manual expression. As a result, the bladder is continuously subjected to the filled state for prolonged time periods and exposed to constant volume overload, which can be speculated to trigger a set of local responses by smooth muscle cells to change their size and orientation as well as gene expression in the early recovery phase of spinal cord injury. The net results, therefore, will be muscular hypertrophy, perhaps with preferred orientation, and increased elastin synthesis over the first few weeks. Later on, after emergence of automatic, involuntary reflex

micturition, the rats will be able to urinate; however, this reflex will be accompanied by bladder-sphincter dyssynergia and detrusor hyperactivity that is mediated by spinal reflex pathways (as described in Section 1) [40]. Thus, when the bladder contracts reflexly, the sphincter also contracts, causing a functional outlet obstruction, and producing a large amount of pressure inside the bladder. The increased pressure will result in high bladder wall stress. The subsequent and constant changes in mechanical environment of the bladder in this phase will, in turn, trigger a different mechanism, such as increased collagen synthesis.

6.3 CONCLUSIONS

Investigating changes in the bladder wall properties through parallel studies such as mechanical testing, protein analyses and histomorphometry, up to 10 weeks after spinal cord injury helped us gain a better understanding of alterations in functional and structural properties of bladder wall and their correlations after SCI. The biomechanical results have demonstrated that the bladder wall exhibits complex biomechanical behaviors that are profoundly altered following SCI. In particular, it was observed that during the initial areflexic phase of SCI the bladder wall undergoes profound remodeling to compensate for increased wall stretch from over-distension. This remodeling process includes increased compliance, mainly due to elastin synthesis and directional smooth muscle hypertrophy. The latter will, in turn, result in an isotropic behavior in short-term (*i.e.* 10-day) SCI bladder samples.

This is then followed by a hyperreflexic phase during which the bladder wall tissue further alters its structure and mechanical behavior, primarily through increase in ECM collagen content and continuous smooth muscle hypertrophy, resulting in an eventual stiffening of the

bladder and reduced bladder compliance in long-term (i.e. 10-week) SCI bladders. The stimuli for these profound functional changes in this phase are presumably different compared to the mechanical stimuli during areflexic phase; large tissue strain during areflexia in contrast to increased tissue stress during hyperreflexia. Therefore, it can be concluded that the functional changes (*e.g.* altered compliance) are direct results of rapid and profound bladder wall tissue remodeling, including changes in smooth muscle cell content and orientation, and collagen and elastin concentrations.

Taken together, it can be concluded that structural changes after spinal cord injury might be part of compensatory mechanisms to protect the organ from the increased mechanical demands on the bladder wall due to prolonged periods of high pressure and/or volume storage in SCI bladders during recovery of the voiding ability. In particular, changes in ECM proteins contributed to adjustment in bladder compliance; increase in elastic fibers immediately after injury resulted in a more compliant bladder wall and increased net collagen content enhanced the bladder wall strength in 10-week SCI specimens. Therefore, the suggested elastin to collagen ratio can be the determining factor to predict the mechanical compliance of the bladder wall tissue. In addition to changes in compliance, alteration in mechanical behavior, such as material class, was also correlated to structural changes in bladder tissue; the orientation of smooth muscle bundles was shown to be responsible for changes in urinary bladder wall tissue material classification. Finally, these results provide first evidence that early and late responses of bladder tissue to the functional changes of the lower urinary tract associated with SCI were distinct.

Further investigations, however, are required to elucidate underlying mechanisms through which the urinary bladder responds to the changes in its mechanical environment. Specifically, the interaction between smooth muscle cells and extracellular matrix proteins need

to be characterized. Moreover, the intrinsic properties of these proteins, including the degree of cross-linking, can play a major role in determining overall mechanical response of the bladder wall tissue, and should be investigated. In addition, active and passive properties of bladder tissue are not well understood and required more investigation, since only inactive characteristics of this tissue has been studied. These new studies, however, may demand new imaging and laboratories approaches. Finally, three-dimensional characterization of bladder wall can be an ultimate task to define structure-function relationship in the urinary bladder wall.

6.4 FUTURE STUDIES

6.4.1 Extended biochemical studies

Despite recent findings, the mechanism of the changes in the tissue composition seen within the bladder after spinal cord injury is unknown, and new approaches are required to address the questions.

6.4.1.1 The role of cross-linking

It has been postulated that the tissue remodeling and changes in mechanical behavior that occurs after similar pathologic conditions such as outlet obstruction could be caused not only by altered collagen concentration in the bladder [84], but also by increased concentration of intermediate filaments such as filamin or desmin [92], altered intrinsic properties of collagen and elastin [93-95], and/or remodeling of cross-bridge elements to reset length-tension relations [96]. Cross-linking, especially, has been discussed quite often in recent literature, since both collagen and elastin are stabilized through covalent crosslinks. There is much evidence showing that

crosslinks of collagen and elastin play an important role in their physiological functions [97-99]. Therefore, they may be thought to be major factors in the presence of abnormalities in various kinds of connective tissue.

6.4.1.2 The role of actin and myosin

On a molecular level, some of the changes observed between diseased and non-diseased bladder wall may be due to active remodeling of the actin protein. There are several types of actin, including, for example, slow and fast actin, which have different properties. As the actin and myosin crossbridges are in series with the forces applied to the tissue, even when the tissue is not contracting and under the relaxing effects of EGTA, any change to the actin molecules will contribute to the differences observed at the tissue level. This may also be an important assay to develop when examining the changes in protein within the bladder wall during disease states.

6.4.1.3 Collagen typing

The tissue remodeling could be caused by an altered ratio of collagen subtypes, which has been observed to occur after mechanical stretch [100], such as what happens in SCI. Kim *et al* [101] reported that bladder outlet obstruction affect on changes of localization and quantity of collagen types as well as collagen content, and these changes lead to bladder remodeling. Moreover, their results suggest that the change in the collagen types rather than the change in the collagen content may have an impact on the bladder function. Uvelius and colleagues [102] also emphasized that collagen concentration could not account entirely for the increased wall stress observed in diseased (*e.g.* obstructed) bladders. They speculated that altered mechanical properties in these bladders could be a result of other changes, for instance, altered conformation

of connective tissue, altered ratio of collagen subtypes, or increased concentration of intermediate filaments.

6.4.2 Diversion Studies

Diversion studies have been performed in which the bladder is constantly emptied through a urine shunt to another organ, preventing pressure and averting volume overload [103]. Even with the shunt, the bladder develops many of the same problems. This suggests that overload is not the sole cause of the dysfunction after spinal cord injury. Identifying the factors that cause the smooth muscle hypertrophy and dyssynergia may, in turn, aid in the development of methods to avoid the dysfunction. Mechanical studies on bladder behavior in diverted rats and other animals with modified neural stimulation may aid in isolating the causes of the changes in structure and tissue behavior.

6.4.3 Active Properties

The passive studies presented here are simpler to perform than those requiring active tissue response. It is known that the mechanical properties of an actively contracting material are not the same as those of the passive material with a larger stiffness. The fundamental behavior of the material is different and must therefore be studied as a separate material. Stimulation of a large piece of tissue such as the 1 cm square samples, either by electrical or chemical means, is much more difficult to perform than uniaxial strip experiments. Some preliminary studies have been performed in this laboratory, but nothing conclusive has been found [79]. In addition, the mechanical properties will be altered in disease states, necessitating further testing.

6.4.4 Morphology studies

Knowledge of bladder morphology is required to understand the impact of disease on bladder function. The studies performed here were not exhaustive, and much is left to be learned. To understand the subtle changes in cross-coupling demonstrated by the quasi-static studies, it is necessary to understand how connective tissue and smooth muscle interact, and how the forces in the bladder wall are distributed between them. One possible method of determining how the tissue-level forces measured in this study relate to the organ-level function may be through the use of computerized tomography or magnetic resonance imaging of the rat bladder before and after disease such as spinal cord injury.

6.4.5 Advanced Modeling

The phenomenological modeling employed here can quantitatively compare parameter differences between these two groups; however, this type of modeling cannot be used to indicate what structural component or components are responsible for the observed changes. A structural constitutive model approach, such as that suggested by Horowitz, et al. [104] for myocardium, in which the muscle fibers connected by collagen fibers were simulated, may be warranted. In this model, both the muscle fibers and collagen fibers have designated direction, distribution, and mechanical properties that were experimentally measured or approximated. It has been recently demonstrated how inclusion of morphological tissue data can result in accurate prediction for planar collagenous tissue using a structural approach [105]. However, detailed and accurate quantitative morphological information about the collagen structure between and within muscle bundles in normal and diseased bladder wall is required before this approach can be effectively implemented.

BIBLIOGRAPHY

1. Hackler, R.H., M.K. Hall, and T.A. Zampieri, *Bladder hypocompliance in the spinal cord injury population*. J Urol, 1989. **141**(6): p. 1390-3.
2. de Groat, W.C., *A neurologic basis for the overactive bladder*. Urology, 1997. **50**(6A Suppl): p. 36-52; discussion 53-6.
3. Mimata, H., et al., *Changes of rat urinary bladder during acute phase of spinal cord injury*. Urol Int, 1993. **51**(2): p. 89-93.
4. Deveaud, C.M., et al., *Molecular analysis of collagens in bladder fibrosis*. J Urol, 1998. **160**(4): p. 1518-27.
5. Ogawa, T., *Bladder deformities in patients with neurogenic bladder dysfunction*. Urol Int, 1991. **47** Suppl 1: p. 59-62.
6. Shin, J.C., et al., *Significance of low compliance bladder in cauda equina injury*. Spinal Cord, 2002. **40**(12): p. 650-5.
7. Weld, K.J., M.J. Graney, and R.R. Dmochowski, *Differences in bladder compliance with time and associations of bladder management with compliance in spinal cord injured patients*. J Urol, 2000. **163**(4): p. 1228-33.
8. Drake, M.J., et al., *Structural and functional denervation of human detrusor after spinal cord injury*. Lab Invest, 2000. **80**(10): p. 1491-9.
9. Kruse, M.N., L.A. Bray, and W.C. de Groat, *Influence of spinal cord injury on the morphology of bladder afferent and efferent neurons*. J Auton Nerv Syst, 1995. **54**(3): p. 215-24.
10. Watanabe, T., D.A. Rivas, and M.B. Chancellor, *Urodynamics of spinal cord injury*. Urol Clin North Am, 1996. **23**(3): p. 459-73.
11. Yoshimura, N., et al., *Pharmacologic and potential biologic interventions to restore bladder function after spinal cord injury*. Curr Opin Neurol, 2000. **13**(6): p. 677-81.
12. Chang, S.L., et al., *Roles of the lamina propria and the detrusor in tension transfer during bladder filling*. Scand J Urol Nephrol Suppl, 1999. **201**: p. 38-45.

13. Koenig, F., et al., *Near-infrared confocal laser scanning microscopy of bladder tissue in vivo*. Urology, 1999. **53**(4): p. 853-7.
14. Murakumo, M., et al., *Three-dimensional arrangement of collagen and elastin fibers in the human urinary bladder: a scanning electron microscopic study*. J Urol, 1995. **154**(1): p. 251-6.
15. Macarak, E.J., et al., *The collagens and their urologic implications*. Adv Exp Med Biol, 1995. **385**: p. 173-7.
16. Gabella, G. and B. Uvelius, *Urinary bladder of rat: fine structure of normal and hypertrophic musculature*. Cell Tissue Res, 1990. **262**(1): p. 67-79.
17. Gloeckner, D.C., *Tissue Biomechanics of the Urinary Bladder Wall*, in *Department of Bioengineering*. 2003, University of Pittsburgh: Pittsburgh. p. 258.
18. Cortivo, R., et al., *Elastin and collagen in the normal and obstructed urinary bladder*. Br J Urol, 1981. **53**(2): p. 134-7.
19. Kim, K.M., et al., *Collagen and elastin in the normal fetal bladder*. J Urol, 1991. **146**(2 (Pt 2)): p. 524-7.
20. Macarak, E.J. and P.S. Howard, *The collagens and their urologic significance*. Scand J Urol Nephrol Suppl, 1997. **184**: p. 25-33.
21. Chang, S.L., et al., *Role of type III collagen in bladder filling*. Neurourol Urodyn, 1998. **17**(2): p. 135-45.
22. Nimni, M.E. and R.D. Harkness, *Molecular structure and functions of collagens.*, in *Collagen Volume I Biochemistry.*, M.E. Nimni, Editor. 1988, CRC Press: Boca Raton, FL.
23. Macarak, E.J. and P.S. Howard, *The role of collagen in bladder filling*. Adv Exp Med Biol, 1999. **462**: p. 215-23.
24. Ewalt, D.H., et al., *Is lamina propria matrix responsible for normal bladder compliance?* J Urol, 1992. **148**(2 Pt 2): p. 544-9.
25. Koo, H.P., et al., *Developmental expression of interstitial collagen genes in fetal bladders*. J Urol, 1997. **158**(3 Pt 1): p. 954-61.
26. Strauss, L., et al., *Distribution of collagen XII and XIV in the bladder wall of the male rat with outlet obstruction*. J Urol, 2000. **163**(4): p. 1304-8.
27. Landau, E.H., et al., *Loss of elasticity in dysfunctional bladders: urodynamic and histochemical correlation*. J Urol, 1994. **152**(2 Pt 2): p. 702-5.

28. Cleary, E.G. and M.A. Gibson, *Elastin-associated microfibrils and microfibrillar proteins*. Int Rev Connect Tissue Res, 1983. **10**: p. 97-209.
29. Rosenbloom, J., et al., *Elastic fibers and their role in bladder extracellular matrix*. Adv Exp Med Biol, 1995. **385**: p. 161-72.
30. Koo, H.P., et al., *Temporal expression of elastic fiber components in bladder development*. Connect Tissue Res, 1998. **37**(1-2): p. 1-11.
31. Ushiki, T. and M. Murakumo, *Scanning electron microscopic studies of tissue elastin components exposed by a KOH-collagenase or simple KOH digestion method*. Arch Histol Cytol, 1991. **54**(4): p. 427-36.
32. Baskin, L.S., et al., *Type III collagen decreases in normal fetal bovine bladder development*. J Urol, 1994. **152**(2 Pt 2): p. 688-91.
33. Coplen, D.E., et al., *Characterization of a fibroblast cell from the urinary bladder wall*. In Vitro Cell Dev Biol Anim, 1994. **30A**(9): p. 604-8.
34. Baskin, L., et al., *Bovine bladder compliance increases with normal fetal development*. J Urol, 1994. **152**(2 Pt 2): p. 692-5; discussion 696-7.
35. Davidson, J.M., K.E. Hill, and J.L. Alford, *Developmental changes in collagen and elastin bioynthesis in the porcine aorta*. Developmental Biology, 1986. **118**: p. 103-111.
36. Macarak, E.J., *Overview of muscle and extracellular matrix in the bladder*. Adv Exp Med Biol, 1999. **462**: p. 117-9.
37. de Groat, W.C., A.M. Booth, and N. Yoshimura, *Neurophysiology of micturition and its modification in animal models of human disease*, in *Nervous Control of the Urogenital System*, C.A. Maggi, Editor. 1993, Harwood Academic Publishers: Chur. p. 227-290.
38. Stover, S.L. and P.R. Fine, *The epidemiology and economics of spinal cord injury*. Paraplegia, 1987. **25**(3): p. 225-8.
39. Stover, S.L., et al., *Iatrogenic dilatation of the upper urinary tract during radiographic evaluation of patients with spinal cord injury*. J Urol, 1986. **135**(1): p. 78-82.
40. de Groat, W.C., et al., *Modification of urinary bladder function after spinal cord injury*. Adv Neurol, 1997. **72**: p. 347-64.
41. Alexander, R.S., *Viscoplasticity of smooth muscle of urinary bladder*. Am J Physiol, 1973. **224**(3): p. 618-22.
42. Coolsaet, B.L.R.A., et al., *Viscoelastic properties of bladder wall strips*. Investigative Urology, 1975. **12**(5): p. 351-355.

43. Coolsaet, B.L.R.A., et al., *Viscoelastic properties of bladder wall strips at constant elongation*. Investigative Urology, 1976. **13**(6): p. 435-440.
44. de Groat, W.C., et al., *A study of synaptic transmission and neuropeptide function in extramural colonic ganglia of the cat*. Nippon Heikatsukin Gakkai Zasshi, 1985. **21** (supplement): p. 95.
45. Weld, K.J. and R.R. Dmochowski, *Association of level of injury and bladder behavior in patients with post-traumatic spinal cord injury*. Urology, 2000. **55**(4): p. 490-4.
46. Alexander, R.S., *Mechanical properties of urinary bladder*. American Journal of Physiology, 1971. **220**(5): p. 1413-1421.
47. van Mastrigt, R., B.L.R.A. Coolsaet, and W.A. van Duyl, *First results of stepwise straining of the human urinary bladder and human bladder strips*. Investigative Urology, 1981. **19**(1): p. 58-61.
48. Damaser, M.S., A. Arner, and B. Uvelius, *Partial outlet obstruction induces chronic distension and increased stiffness of rat urinary bladder*. NeuroUrol Urodyn, 1996. **15**(6): p. 650-65.
49. Dean, G.E., et al., *Active and passive compliance of the fetal bovine bladder*. J Urol, 1997. **158**(3 Pt 2): p. 1094-9.
50. Dahms, S.E., et al., *Composition and biomechanical properties of the bladder acellular matrix graft: comparative analysis in rat, pig and human*. Br J Urol, 1998. **82**(3): p. 411-9.
51. Watanabe, H., et al., *A finite deformation theory of intravesical pressure and mural stress of the urinary bladder*. Journal of Experimental Medicine, 1981. **135**: p. 301-307.
52. Alexander, R.S., *Series elasticity of urinary bladder smooth muscle*. Am J Physiol, 1976. **231**(5 Pt. 1): p. 1337-42.
53. Rohrmann, D., et al., *Compliance of the obstructed fetal rabbit bladder*. NeuroUrol Urodyn, 1997. **16**(3): p. 179-89.
54. Coplen, D.E., E.J. Macarak, and R.M. Levin, *Developmental changes in normal fetal bovine whole bladder physiology*. J Urol, 1994. **151**(5): p. 1391-5.
55. Levin, R.M., P. Horan, and S.P. Liu, *Metabolic aspects of urinary bladder filling*. Scand J Urol Nephrol Suppl, 1999. **201**: p. 59-66.
56. van Mastrigt, R., B.L.R.A. Coolsaet, and W.A. van Duyl, *The passive properties of the urinary bladder in the collection phase*. Urologia Internationali, 1978. **33**: p. 14-21.

57. Damaser, M.S., *Whole bladder mechanics during filling*. Scand J Urol Nephrol Suppl, 1999. **201**: p. 51-8.
58. Gloeckner, D.C., et al., *Passive biaxial mechanical properties of the rat bladder wall after spinal cord injury*. J Urol, 2002. **167**(5): p. 2247-52.
59. Sacks, M., et al., *Loss of flexural rigidity in bioprosthetic heart valves with fatigue: New findings and the relation to collagen damage*. Journal of Biomechanical Engineering, submitted.
60. Nagatomi, J., et al., *Changes in the biaxial viscoelastic response of the urinary bladder following spinal cord injury*. Ann Biomed Eng, 2004. **32**(10): p. 1409-19.
61. Klevmark, B., *Natural pressure-volume curves and conventional cystometry*. Scand J Urol Nephrol Suppl, 1999. **201**: p. 1-4.
62. Zermann, D.H., et al., *Diagnostic value of natural fill cystometry in neurogenic bladder in children*. Eur Urol, 1997. **32**(2): p. 223-8.
63. Andersson, S., A. Kronström, and P. Bjerle, *Viscoelastic properties of the normal human bladder*. Scandanavian Journal of Urological Nephrology, 1989. **23**: p. 115-120.
64. Kondo, A., J.G. Susset, and J. Lefavre, *Viscoelastic properties of bladder I. Mechanical model and its mathematical analysis*. Investigative Urology, 1972. **10**(2): p. 154-163.
65. van Mastrigt, R. and J.C. Nagtegaal, *Dependence of the viscoelastic response of the urinary bladder wall on strain rate*. Med Biol Eng Comput, 1981. **19**(3): p. 291-6.
66. Salinas, J., et al., *A study on the viscoelastic properties of the urinary bladder in dogs*. Urol Int, 1992. **49**(4): p. 185-90.
67. Tözeren, A., *Assessment of fiber strength in a urinary bladder by using experimental pressure volume curves: an analytical method*. Journal of Biomechanical Engineering, 1986. **108**: p. 301-305.
68. Damaser, M.S., et al., *The concept of bladder work: work and power in bladder emptying*. Scand J Urol Nephrol Suppl, 1997. **184**: p. 35-41.
69. Bross, S., et al., *Combined evaluation of detrusor pressure and bladder wall thickness as a parameter for the assessment of detrusor function: an experimental in vivo study*. J Urol, 2001. **166**(3): p. 1130-5.
70. Abbey, J.C. and L. Close, *Electrical impedance measurement of urinary bladder fullness*. J Microw Power, 1983. **18**(3): p. 305-9.

71. Ozawa, H., et al., *Development of noninvasive velocity flow video urodynamics using Doppler sonography. Part I: Experimental urethra [see comments]*. J Urol, 1998. **160**(5): p. 1787-91.
72. Ozawa, H., et al., *Development of noninvasive velocity flow video urodynamics using Doppler sonography. Part II: clinical application in bladder outlet obstruction [see comments]*. J Urol, 1998. **160**(5): p. 1792-6.
73. Coolsaet, B.L.R.A., et al., *Visco-elastic properties of the bladder wall*. Urologia Internationali, 1975. **30**: p. 16-26.
74. Koo, H.P., et al., *The ontogeny of bladder function in the fetal calf*. J Urol, 1995. **154**(1): p. 283-7.
75. Finkbeiner, A.E., *In vitro responses of detrusor smooth muscle to stretch and relaxation*. Scand J Urol Nephrol Suppl, 1999. **201**: p. 5-11.
76. Sacks, M.S., *Biaxial mechanical evaluation of planar biological materials*. Journal of Elasticity, 2000. **61**: p. 199-246.
77. Billiar, K.L. and M.S. Sacks, *Biaxial mechanical properties of the natural and glutaraldehyde treated aortic valve cusp--Part I: Experimental results*. Journal of Biomechanical Engineering, 2000. **122**(1): p. 23-30.
78. Nagatomi, J., M. Chancellor, and M. Sacks. *Active Biaxial Mechanical Properties of Bladder Wall Tissue*. in *ASME IMECE '03*. 2003. Washington D.C.
79. Gloeckner, D.C., et al. *Active biaxial mechanical response of the urinary bladder wall*. in *American Society of Mechanical Engineering Summer Bioengineering Conference*. 2001. Snowbird, Utah.
80. Fung, Y.C., *Biomechanics: Mechanical Properties of Living Tissues*. 2nd ed. 1993, New York: Springer Verlag. 568.
81. Nagatomi, J., et al., *Quantification of bladder smooth muscle orientation in normal and spinal cord injured rats*. Ann Biomed Eng, 2005. **33**(8): p. 1078-89.
82. Desmouliere, A., I.A. Darby, and G. Gabbiani, *Normal and pathologic soft tissue remodeling: role of the myofibroblast, with special emphasis on liver and kidney fibrosis*. Lab Invest, 2003. **83**(12): p. 1689-707.
83. Nagatomi, J., et al., *Early molecular-level changes in rat bladder wall tissue following spinal cord injury*. Biochem Biophys Res Commun, 2005. **334**(4): p. 1159-64.
84. Uvelius, B. and A. Mattiasson, *Collagen content in the rat urinary bladder subjected to infravesical outflow obstruction*. J Urol, 1984. **132**(3): p. 587-90.

85. Kim, K.M., et al., *Collagen and elastin in the obstructed fetal bladder*. J Urol, 1991. **146**(2 (Pt 2)): p. 528-31.
86. Byrne, D.S., et al., *Effect of intravesical capsaicin and vehicle on bladder integrity control and spinal cord injured rats*. J Urol, 1998. **159**(3): p. 1074-8.
87. Chancellor, M.B., et al., *Micturition patterns after spinal trauma as a measure of autonomic functional recovery*. J Urol, 1994. **151**(1): p. 250-4.
88. Sun, W., et al., *Biaxial mechanical response of bioprosthetic heart valve biomaterials to high in-plane shear*. Journal Biomechanical Engineering, 2003. **125**: p. 372-380.
89. Criscione, J.C., M.S. Sacks, and W.C. Hunter, *Experimentally tractable, pseudo-elastic constitutive law for biomembranes: I. Theory*. J Biomech Eng, 2003. **125**(1): p. 94-9.
90. Kondo, A. and J.G. Susset, *Viscoelastic properties of bladder*. Investigative Urology, 1974. **11**(6): p. 459-465.
91. Sandberg, L.B., N.T. Soskel, and J.G. Leslie, *Elastin structure, biosynthesis, and relation to disease states*. New England Journal of Medicine, 1981. **304**(10): p. 566-579.
92. Malmqvist, U., A. Arner, and B. Uvelius, *Cytoskeletal and contractile proteins in detrusor smooth muscle from bladders with outlet obstruction--a comparative study in rat and man*. Scandinavian Journal of Urology and Nephrology, 1991. **25**(4): p. 261-7.
93. Elbadawi, A., *Voiding dysfunction in benign prostatic hyperplasia: trends, controversies and recent revelations. II. Pathology and pathophysiology*. Urology, 1998. **51**(5A Suppl): p. 73-82.
94. Elbadawi, A., *Functional pathology of urinary bladder muscularis: the new frontier in diagnostic uropathology*. Semin Diagn Pathol, 1993. **10**(4): p. 314-54.
95. Gosling, J.A., *Modification of bladder structure in response to outflow obstruction and ageing*. Eur Urol, 1997. **32 Suppl 1**: p. 9-14.
96. Mattiasson, A. and B. Uvelius, *Changes in contractile properties in hypertrophic rat urinary bladder*. J Urol, 1982. **128**(6): p. 1340-2.
97. Bailey, A.J., et al., *Biochemical changes in the collagen of human osteoporotic bone matrix*. Connect Tissue Res, 1993. **29**(2): p. 119-32.
98. Masse, P.G., et al., *Pyridoxine deficiency affects biomechanical properties of chick tibial bone*. Bone, 1996. **18**(6): p. 567-74.
99. Stone, P.J., et al., *Cross-linked elastin and collagen degradation products in the urine of patients with scleroderma*. Arthritis Rheum, 1995. **38**(4): p. 517-24.

100. Baskin, L., P.S. Howard, and E. Macarak, *Effect of mechanical forces on extracellular matrix synthesis by bovine urethral fibroblasts in vitro*. J Urol, 1993. **150**(2 Pt 2): p. 637-41.
101. Kim, J.C., et al., *Effects of partial bladder outlet obstruction and its relief on types I and III collagen and detrusor contractility in the rat*. Neurorol Urodyn, 2000. **19**(1): p. 29-42.
102. Uvelius, B., P. Lindner, and A. Mattiasson, *Collagen content in the rat urinary bladder following removal of an experimental infravesical outlet obstruction*. Urologia Internationalis, 1991. **47**(4): p. 245-9.
103. Kruse, M.N., B. Bennett, and W.C. De Groat, *Effect of urinary diversion on the recovery of micturition reflexes after spinal cord injury in the rat*. J Urol, 1994. **151**(4): p. 1088-91.
104. Horowitz, A., et al., *Structural Three Dimensional Constitutive Law for the Passive Myocardium*. Journal of Biomechanical Engineering, 1988. **110**: p. 200-207.
105. Sacks, M.S., *Incorporation of experimentally-derived fiber orientation into a structural constitutive model for planar collagenous tissues*. J Biomech Eng, 2003. **125**(2): p. 280-7.